Supporting Information for:

DEVELOPMENT OF IODINATED INDOCYANINE GREEN ANALOGS AS A STRATEGY FOR TARGETED THERAPY OF LIVER CANCER

Sierra C. Marker[§,1] Andres F. Espinoza[§,2] A. Paden King,[3] Sarah Woodfield,[2] Roma Patel,[2] Kwamena Baidoo,[3] Meredith N. Nix,[4] Larissa Miasiro Ciaramicoli,[5] Young-Tae Chang,[5*] Freddy E. Escorcia*,[3] Sanjeev A. Vasudevan*,[2] Martin J. Schnermann*[1]

[1]Chemical Biology Laboratory, Center for Cancer Research, National Cancer Institute, National Institutes of Health, Frederick, Maryland 21702, United States

[2]Divisions of Pediatric Surgery and Surgical Research, Michael E. DeBakey Department of Surgery, Pediatric Surgical Oncology Laboratory, Texas Children's Surgical Oncology Program and Liver Tumor Program, Dan L. Duncan Cancer Center, Baylor College of Medicine, Houston, Texas 77030, United States

[3]Molecular Imaging Branch, Center for Cancer Research, National Cancer Institute, National Institutes of Health, Bethesda, Maryland 20852, United States

[4]Department of Chemistry, Pohang University of Science and Technology (POSTECH), Pohang Gyeongbuk, 37673, Republic of Korea

CONTENT

EXPERIMENTAL SECTION

Methods and Materials. All reactions were carried out under an inert atmosphere. Reagents were purchased at a high commercial quality (typically 97% or higher) and used without further purification, unless otherwise stated. Commercially available ICG (Cayman Chemical, Ann Arbor, MI) was used for these studies. ^{1}H NMR spectra were recorded on a 400 MHz Bruker spectrometer and are reported relative to deuterated solvent signals (MeOH-d_4: ^{1}H NMR = 3.30). The following abbreviations were used to explain the multiplicities: s = singlet, d = doublet, t = triplet, q = quartet, dd = double doublet, m = multiplet. Electrospray ionization mass spectrometry (ESI-MS) data were collected on triple-stage quadrupole instrument in a positive mode. Flash column chromatography was performed using reversed phase (100 Å, 20–40-micron particle size, RediSep® Rf Gold® Reversed-phase C18 or C18Aq) and silica on a CombiFlash® Rf 200i (Teledyne Isco, Inc.). LC/MS was performed using a Shimadzu LCMS-2020 Single Quadrupole utilizing a Kinetex 2.6 µm C18 100 Å (2.1 x 50 mm) column obtained from Phenomenex, Inc (Torrance, CA). Runs employed a gradient of 0-90% MeCN/H_2O with 0.05% formic acid over 4.5 min at a flow rate of 0.2 mL/min. Preparatory HPLC was performed on Waters HPLC equipped with Waters 515 HPLC Pump, Water 2998 Photodiode Array Detector, Waters 2545 Binary Gradient Module and Waters 2767 Sample Manager. The HPLC was installed with Luna 10 µm C18 column (100 x 30 mm) and each run employed 10-95% or 60-95% MeCN/H_2O gradient with 0.1% TFA over 10 mins. Analytical HPLC analyses were collected from Agilent Infinity 1260 II Quaternary LC module using TSK-Gel Octadecyl 4-PW (7 µm, 4.6 x 150 mm) column in 5-95% CH_3CN/water gradient with 0.1% trifluoroacetic acid (0.5 mL/min) over 20 minutes. All statistical analyses were carried out by GraphPad Prism version 9.0 (GraphPad Software). No unexpected or unusually high safety hazards were encountered.

Synthesis of iodo indoles (1). All iodo indoles were synthesized through a previously reported procedure,[1] with the exception of the 5′-iodo indole, which was purchased from Ambeed, Inc. **S1** (200 mg, 0.70 mmol) was then treated with 1,4-butane sultone (**S2**, 287 mg, 2.10 mmol) at 110 °C for 24 h. The alkylated indoles, **1**, were then directly used without purification.

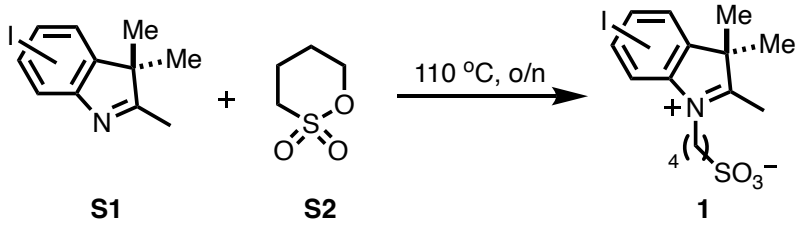

S1 **S2** **1**

Synthesis of 2. The pyridinium salt was synthesized via a previously reported procedure.[2]

Synthesis of 4-mono-I-ICG (3). To a 20 mL microwave vial **S3** (135 mg, 0.38 mmol), **2** (150 mg, 0.76 mmol), and NaOAc (125 mg, 1.52 mmol) were added sequentially in 15 mL of absolute ethanol. The reaction mixture stirred at room temperature for 15 min. The crude reaction mixture was purified on C18 reversed phase chromatography (10–70% CH_3CN+0.1% TFA/H_2O+0.1% TFA) to produce **S4** as a blue-purple solid (53 mg, 26%).

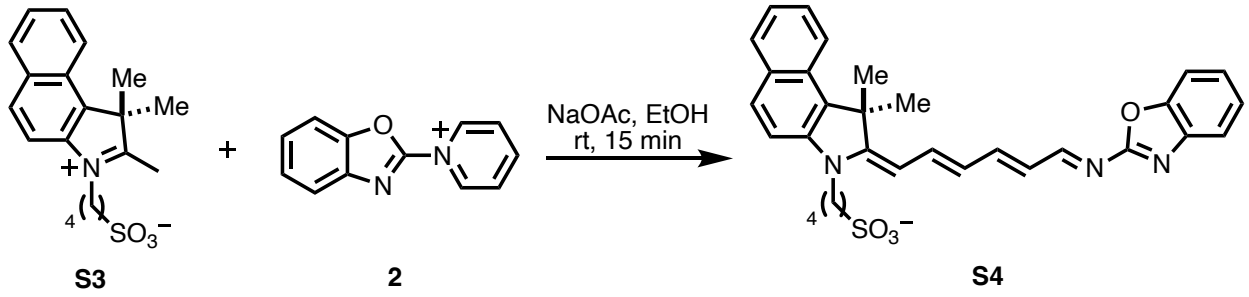

S3 **2** **S4**

To a 10 mL microwave vial **1** (27 mg, 0.06 mmol) and **S4** (20 mg, 0.04 mmol) were combined in 0.4 mL of MeOH. Then, TEA (9 µL, 0.06 mmol) and acetic anhydride (9 µL, 0.09 mmol) were added, sequentially. The reaction mixture stirred at room temperature for 24 h. The solvent was removed, and the crude reaction mixture was purified on C18 reversed phase chromatography (10–70% CH_3CN+0.1% TFA/H_2O+0.1% TFA) to produce **3** as a blue-green solid (12 mg, 39%).

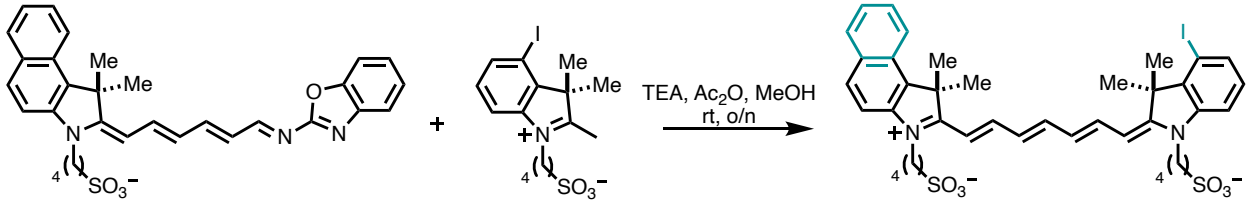

S4 **1** **3**

^{1}H NMR (400 MHz, Methanol-d_4) δ 8.27 (d, 1H, J = 8.62 Hz), 8.10 (t, 1H), 8.06–8.01 (m, 2H), 7.80 (t, 1H), 7.73–7.50 (m, 5H), 7.24 (d, 1H, J = 8.15 Hz), 7.07 (t, 1H), 6.70–6.57 (m, 3H), 6.15 (d, 1H, J = 13.50 Hz), 4.35 (t, 2H), 4.01 (m, 2H), 2.91 (m, 4H), 2.05–1.93 (m, 14H), 1.83 (s, 6H). HRMS (ESI) calculated for $C_{39}H_{46}IN_2O_6S_2^+$ $(M)^-$ 829.1837, observed 829.1847.

Synthesis of 4-I-ICG (4). To a 20 mL microwave vial **1** (440 mg, 0.97 mmol), **2** (97 mg, 0.49 mmol), and NaOAc (120 mg, 1.46 mmol) were added sequentially in 4 mL of absolute ethanol. The reaction mixture was heated at 60 °C for 1 h. The flask was cooled to room temperature and solvent was removed. The crude reaction mixture was purified on C18 reversed phase chromatography (10–70% CH_3CN+0.05% formic acid/H_2O) to produce **4** as a blue-green solid (150 mg, 34%).

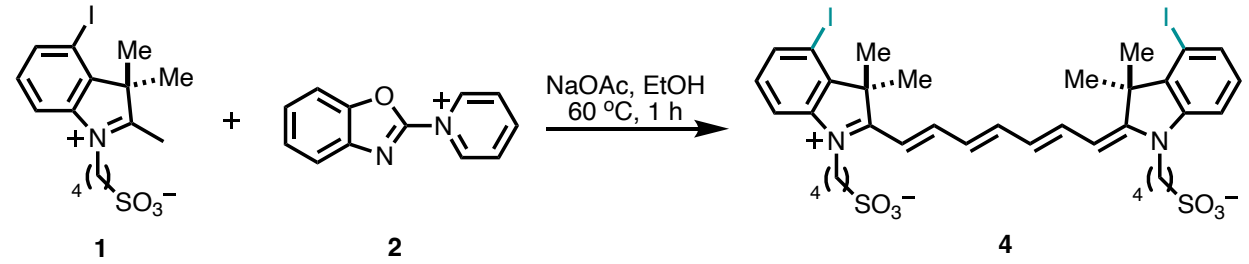

1 2 4

^{1}H NMR (400 MHz, Methanol-d_4) δ 7.96 (t, 2H), 7.65 (d, 3H, J = 7.89 Hz), 7.38 (d, 2H, J = 7.89 Hz), 7.13 (t, 2H), 4.11, (t, 4H), 2.89 (t, 4H), 1.95 (m, 8H), 1.80 (s, 12H). HRMS (ESI) calculated for $C_{35}H_{43}I_2N_2O_6S_2^+$ $(M)^-$ 905.0647, observed 905.0638.

Synthesis of 5-I-ICG (5). To a 20 mL microwave vial **1** (250 mg, 0.59 mmol), **2** (60 mg, 0.30 mmol), and NaOAc (73 mg, 0.89 mmol) were added sequentially in 2 mL of absolute ethanol. The reaction mixture was heated at 60 °C for 1 h. The flask was cooled to room temperature and solvent was removed. The crude reaction mixture was purified on C18 reversed phase chromatography (10–70% CH_3CN+0.05% formic acid/H_2O) to produce **5** as a blue-green solid (125 mg, 58%).

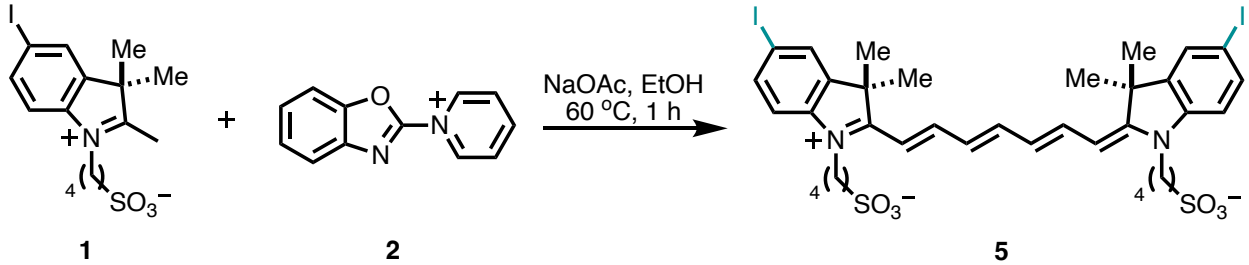

1 2 5

^{1}H NMR (400 MHz, Methanol-d_4) δ 7.92 (t, 2H), 7.79 (s, 2H), 7.73 (d, 2H, J = 8.42 Hz), 7.60 (m, 1H), 7.14 (d, 2H, J = 8.42 Hz), 6.61 (t, 2H), 6.36 (d, 2H, J = 14.10 Hz), 4.08 (t, 4H), 2.88 (t, 4H), 1.94 (m, 8H), 1.68 (s, 12H). HRMS (ESI) calculated for $C_{35}H_{43}I_2N_2O_6S_2^+$ $(M)^-$ 905.0647, observed 905.0640.

Synthesis of 6-I-ICG (6). To a 20 mL microwave vial **1** (205 mg, 0.49 mmol), **2** (47 mg, 0.24 mmol), and NaOAc (60 mg, 0.73 mmol) were added sequentially in 2 mL of absolute ethanol. The reaction mixture was heated at 60 °C for 1 h. The flask was cooled to room temperature and solvent was removed. The crude reaction mixture was purified on C18 reversed phase chromatography (10–70% CH_3CN+0.05% formic acid/H_2O) to produce **6** as a blue-green solid (90 mg, 33%).

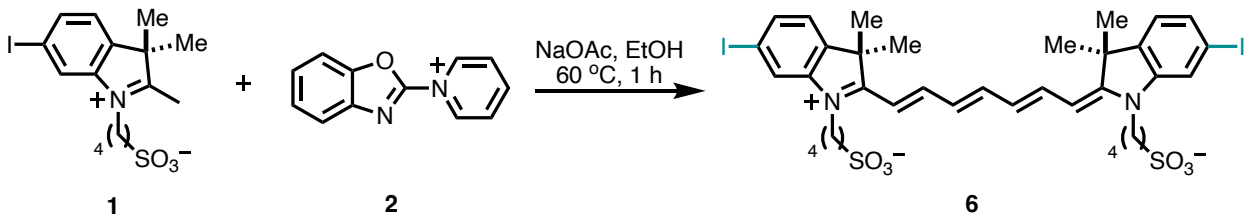

1 2 6

^{1}H NMR (400 MHz, Methanol-d_4) δ 7.94–7.91 (m, 2 H), 7.66 (s, 2H), 7.57 (d, 2H, J = 7.86 Hz), 7.24 (d, 2H, J = 7.86 Hz), 6.62 (t, 2H), 6.38 (d, 2H, J = 13.38 Hz),[1] 4.08 (m, 4H), 2.90 (t, 4H), 1.93 (t, 8H), 1.67 (s, 12H). HRMS (ESI) calculated for $C_{35}H_{43}I_2N_2O_6S_2^+$ $(M)^-$ 905.0647, observed 905.0642.

Absorbance Measurements. Absorbance curves were obtained on a Jasco V-770 spectrophotometer. Extinction coefficients (ε) were determined in water or phosphate-buffered saline (PBS) pH 7.2 containing 10 mg/mL bovine serum albumin (BSA) using Beer's law, from plots of absorbance vs. concentration (1–10 μM). Spectra were recorded with disposable micro-UV-Cuvette holder with 10 mm path length. At least three independent readings were taken at each concentration.

Emission Quantum Yields. Absolute fluorescence quantum yields (Φ_F) were measured in water or phosphate-buffered saline (PBS) pH 7.2 containing 10 mg/mL bovine serum albumin (BSA) using a Horiba fluorimeter QM-8075-11-C equipped with R928 PMT point detector and an integrating sphere to determine photons absorbed and emitted by a sample. Measurements were carried out at concentrations with optical density of less than 0.1 and self-absorption corrections were performed using the instrument software.

CRISPR Screen. *Cell culture.* HeLa (cervical cancer) cells and derivatives (dCas9-VPR HeLa and SLC-CRISPRa pools) were cultured in Dulbecco's Modified Eagle's Medium (DMEM) supplemented with 10% fetal bovine serum (FBS, Atlas Biologicals) and 1% penicillin-streptomycin (Welgene) at 37°C in an atmosphere of 5% CO_2. Indocyanine green (ICG) dye was dissolved in dimethyl sulfoxide (DMSO) and diluted in complete DMEM for FACS and flow cytometry for Figure 2. ICG dye was dissolved in water and diluted in complete MEM for flow cytometry.

SLC-CRISPRa pool design. Procedures to generate SLC-CRISPRa pools from sgRNA library design and lentiviral production follow a previously described procedure.[3] Briefly, a library containing 3800 sg-RNA was selected from NCBI database (https://www.ncbi.nlm.nih.gov/gene) targeting 380 human solute carrier transporter (SLC) genes. A dCas9-VPR combined with three types of transcription activation domains were transfected in HeLa cells (ATCC® CCL-2™) to create a stable cell line capable of enhancing gene transcription. SLC-CRISPRa pools were finally generated by lentiviral transfection of the 3800 sgRNA library in dCas9-VPR HeLa cells, purified with puromycin (2 μg/mL).

Flow cytometry and FACS analysis. Subcultures of SLC-CRISPRa pools were prepared over 1.5x10^6 cells/plate to secure SLC genes. The cells were incubated with complete media (DMEM/10%FBS/1%PS) with ICG (10 μM) for 30 min at 37°C, as the confluency achieved >80%. After removal of the ICG containing media, the cells were detached using trypsin-EDTA (Welgene), washed with Dulbecco's PBS (Simply) and subsequently kept in normal culture media (4°C) for flow cytometry and cell sorting. Live cell gates were made with FSC-A/SSC-A for the exclusion of debris, followed by single-cell gating with FSC-H/FSC-A and acquisition of 10,000 events by flow cytometry. The top 3% brightest population of the fluorescence intensity was sorted by S3e Cell Sorter (Bio-Rad) and cultured for one week to allow cell expansion before the next round. FlowJo™ Software was used for flow cytometry and sorting analysis.[3]

[1] These protons integrate to less than 2 due to hydrogen-deuterium exchange, which has been observed with related molecules in prior work.

Next-generation sequencing (NGS). After enrichment of more than 99% of the sorted cells compared to the original pool, 5th round sorted cells were subjected to NGS. Genomic DNA was isolated according to the procedures described in QIAamp® DNA Mini Kit (QIAGEN) for DNA purification through spin protocol.

Cloning. A cell dilution technique was applied to obtain CRISPR-targeted cell clones from the enriched 5th round sorted cells. After diluting 5 cells/mL, 100 µL was pipetted into each well of a 96-well plate to achieve the ratio of 1 cell/2 wells. One week later, wells containing only one cell were selected for and expanded into a 10-cm dish. To confirm the expression of each transporter, RT-PCR, flow cytometry, and imaging were performed.

RT-PCR. Total RNA was extracted using RNeasy® Mini Kit (QIAGEN) as described in the RNeasy Mini Handbook for purification of animal cells using spin technology from cultured cells. Quantitative RT-PCR was performed by StepOne™ Real-Time PCR system by using Power SYBR™ Green RNA-to-C_T™ *1-Step* Kit (Applied Biosystems™) in q-TOWER^{3}G (Analytik Jena AG 2020©). Relative mRNA expression of selected SLC genes was normalized by β-actin. The sequences analyzed by RT-PCR were selected from the top six enriched genes listed from the NGS data of the enriched cell population. Three gene sequences were later selected and compared in clones to identify the purified populations of SLC25A15, SLCO1B3, and SLC4A11 (verified using flow cytometry and confocal fluorescence imaging). The primers sequences are as described:

β-actin:

F–5′-GGATGCAGAAGGAGATCACTG-3′

R–5′-CGATCCACACGGAGTACTTG-3′

SLC25A15:

F–5′-AGGCCTTAGCCTCCCAACAAGGTC-3′

R–5′-GGAGGCCGACAACCCCGAGA-3′

SLCO1B3:

F–5′-GGATGGACTTGTTGCAGTTG -3′

R–5′-TTAGTTGGCAGCAGCATTGT-3′

SLC8B1:

F–5′-CGTGCTGGTTACCACAGTGG -3′

R–5′-CTTCCGTGGCAGGGTCAG-3′

SLC4A11:

F–5′- TCAATGTCAACCTTGAGATGCAG-3’

R–5′-TCAGGTACTTTCGGGAGGTGT-3′

SLC5A12:

F–5′-TCCACAATGTATTAGAGCAAT-3′

R–5′-ATAGATTCCGAGCCAAGTA-3′

Confocal fluorescence imaging. Clone images were taken using an Operetta CLS (PerkinElmer). The attached cells in a 96-well plate were incubated with ICG (10 µM) in complete DMEM for 30 min at 37°C. After washing with PBS, cells were supplemented with PBS (1% FBS) prior to imaging.

Cell Culture. All cells were grown at 37°C in an atmosphere of 5% CO_2. Cells in Figure 3, HEK-293T (healthy kidney), HepG2 (pediatric hepatoblastoma), Hep3B (pediatric hepatocellular carcinoma), and Huh-7 (adult hepatocellular carcinoma) cells were purchased from American Type Culture Collection (ATCC, Manassas, VA, USA) and grown in Dulbecco’s Modified Eagle’s Medium (DMEM) supplemented with 10% fetal bovine serum (FBS), 2 mM L-glutamine, 100

units/mL penicillin, and 100 μg/mL streptomycin (complete MEM). OATP1B3 HEK-293T (transfected healthy kidney) cells were grown in complete phenol red-free DMEM with 5 μg/mL puromycin and established in our laboratory as described below. Cells were passed at 80−90% confluence using trypsin/EDTA. Cells were tested monthly for mycoplasma contamination with the PlasmoTest mycoplasma detection kit from InvivoGen.

Cells in **Figure S20**, HepG2 cells were commercially acquired (HepG2, ATCC, Manassas, VA, USA). SH-SY5Y were generously provided by Jianhua Yang (Baylor College of Medicine, Houston, TX, USA). Hep G2 and SH-SY5Y were cultured in Eagle's Minimum Essential Medium (EMEM, Lonza, Allendale, NJ, USA) supplemented with 10% heat-inactivated fetal bovine serum (FBS, SAFC Biosciences, Lenexa, KS, USA), 2 mM glutamine (Invitrogen, Carlsbad, CA, USA), and 100 units/ml streptomycin/penicillin (Invitrogen).

HB17 patient-derived cell line was established in our laboratory. After obtaining tissue we plated the dissociated cells in Corning Matrigel GFR Membrane Matrix (Fisher Scientific), Hampton, NH) coated 6 cm culture plates and passaged every 2 weeks. After 20 passages we were able to wean the need for Matrigel. By passage 40 we were able to solely maintain HB17 in MEM and HBM media (Lonza, Walkerville, MD) in 1:1 ratio. For the experiments in **Figure S20** we used passage # 42. HB17 was compared to the original patient tumor and validated through STR assay, RNA sequencing, and IHC. The cell culture media and supplements were purchased from Thermo Fisher Scientific.

Lentiviral Transduction. HEK-293T cells (50,000 cells) were plated into 24-well plates in complete DMEM. On day 2, the cells were washed with PBS and incubated with complete DMEM (no pen/strep) containing polybrene (8 μg/mL). Lentivirus (Lenti-CMV-SLCO1c1v1, Vigene LH890109, 1.94 x 10^8 TU/mL; or Lenti-CMV-SLCO1B3, Vigene LH823331, 1.68 x 10^8 TU/mL) was added to result in multiplicity of infections (MOIs) of 0, 1, 2.5, 5, or 10. On day 3, the media was removed and 500 μL of complete media containing puromycin (1 μg/mL) was added. On day 6, cells were washed with the puromycin-containing media and fresh puromycin-containing media was added. On day 8, cells were passaged into a 6-well plate and continued to grow with puromycin-containing media (2 mL). On day 10, cells were washed with media. On day 13, cells were trypsinized and transferred to a T75 flask and grown with media containing 0.5 μg/mL puromycin. On day 15, cells were switched to complete media containing pen/strep and passaged normally. All lentiviral cell lines were grown with phenol red-free media containing 0.5 μg/mL of puromycin to ensure stable transfection.

Immunoblotting. Cells were lysed in TBS buffer (50 mM Tris, pH 7.5, 150 mM NaCl, 1 mM EDTA) containing 1% Triton X-100, 2 U/ml DNase and protease inhibitor cocktail tablet (Cell Signaling). To quantify protein levels, a Pierce BCA Protein Assay kit was used. The lysates were incubated on ice for 30 min, followed by heating for 10 min in SDS-PAGE sample buffer (50 mM Tris (pH 6.8), 100 mM dithiothreitol, 2% SDS, 0.1% bromophenol blue, 10% glycerol). Proteins were separated on SDS-PAGE and transferred to PVDF membranes (Fisher). Membranes were blocked in TBS containing 5% bovine serum albumin and 0.1% Tween-20 for 1 h, followed by incubation with the primary antibody SLCO1B3 (Atlas AMAb91231) or β-actin (Cell Signaling) overnight at 4 °C. After incubation with the horseradish peroxidase-coupled secondary antibody at room temperature for 1 h, immunoblots were visualized using enhanced chemiluminescence (ECLPlus, GE Healthcare). The blot was imaged on a Bio-Rad ChemiDoc MP Imaging System.

Fluorescence Microscopy. For **Figures 3** and **S6**, HepG2, Hep3B, HEK-293T, OATP1B3 HEK-293T (MOI 10), and lenti-control OATP1c1.v1 HEK-293T cells were plated in 10-well chamber plates and incubated for 24 hours. Cells were fixed at room temperature for 15 minutes using 4% paraformaldehyde in 1X PBS (pH 7.2). Cells were washed 3x with PBS pH 7.2. Cells were permeabilized in PBS-Triton (0.1% Triton X) for 20 minutes. Cells were then blocked with blocking buffer (5% goat serum, 0.1% Triton X-100 in PBS) for 1 hour at room temperature on a shaker. Buffer was removed and 100 µL of primary antibody (1:100, Atlas AMAb91231 anti-SLCO1B3, 0.3 mg/mL) in antibody dilution buffer (1% goat serum, 0.1% Triton X-100 in PBS) was added to each well and incubated overnight at 4°C. Cells were washed 3 x 20 minutes in PBS and then incubated with the secondary antibody in antibody dilution buffer (1:100, goat anti-mouse IgG (H+L) cross-adsorbed secondary antibody, AlexaFluor-488, 2 mg/mL) for 1 hour in the dark at room temperature on a shaker. Cells were washed 3 x 20 minutes with PBS and then incubated for 10 minutes with DAPI. Cells were washed 3x with PBS, then imaged in Hank's Buffered Saline Solution (HBSS) using the Andor spinning disk confocal microscope with a Lecia DMi8 base and 63x oil immersed objective with a 488 nm laser at 100% laser power for 500 ms. Fiji was used for image processing.

For **Figure S20**, HepG2, SH-SY5Y, and HB17 cells were plated in 10 cm wells and incubated with 25µM of ICG (diluted in water) for 1 hour. Cells were then washed 3x with PBS pH 7.2. Cells were then washed 1x daily with PBS. Cells were fixed at room temperature using 4% paraformaldehyde in 1X PBS (pH 7.2). After 72 hours cells, brightfield images of cells and fluorescent microscope images were taken on a BZ-X710 All-in-One Fluorescence Microscope (Keyence, Itasca, IL, USA) at the indicated magnifications and scales with ICG and brightfield filters.

Flow Cytometry. HepG2, Hep3B, Huh-7, HEK-293T, lenti-control OATP1c1.v1 HEK-293T, and OATP1B3 HEK-293T (MOI 10) cells were detached using trypsin and split into 15 mL falcon tubes (500,000 cells/tube). Cells were treated with 10 µM of ICG or I-ICG compounds in DMEM with 10% FBS for 1 h at 37°C. Cells were centrifuged for 5 minutes at 200 g and the media was removed and replaced with fresh media for 1 h at 37°C. Cells were centrifuged for 5 minutes at 200 g and washed 3x with PBS pH 7.2 containing 0.2% BSA and kept on ice during washes. The cells were then resuspended in PBS/BSA and fluorescence intensity was analyzed on a BD LSRII Fortessa^{TM} instrument using a 633 nm laser and APC-Cy7 emission (780/60 nm). Analysis was performed using FlowJo vs 10.8.0.

For **Figures S16–S19**, HepG2, HB17, and SH-SY5Y cell lines were fixed using 4% paraformaldehyde and analyzed with standard flow cytometry on a Symphony instrument (BD Biosciences) using a 637 nm laser to excite ICG and 4-I-ICG with a 780/60 nm bandpass filter for detection and a 405 nm laser was used to excite DAPI with a 431/28 bandpass filter for detection. FSC and SSC were used to discriminate cell debris and 2 singlet discriminators were used to remove cells that adhered together as shown. DAPI was used to extract dead cells. ICG signal was measured after removal of cell clumps and dead cells.

Animal and IVIS Imaging with Hep3B and Huh-7 Tumor Xenograft Protocol. All procedures associated with these experiments were approved by the Institutional Care and Use Committee of

the National Institutes of Health under protocol ROB-104. These studies were performed using 8-12-week-old athymic nude mice (Frederick National Laboratory, Frederick, MD). Mice were implanted with 2.5 x 10^6 cells in 200 μL of a 1:1 mixture of Matrigel (Corning, Corning, NY) and cell culture media. Once tumors reached at least 100 mm^3, mice were injected with 2 mg/kg of ICG or I-ICG and imaged using an IVIS Lumina system after 4, 24, and 48 h. Following the final time point, mice were euthanized by CO_2 asphyxiation, dissected, and their tumors and livers were imaged *ex vivo*.

Animal and Patient-Derived Xenograft Protocol. All animal procedures used in this study were performed under an animal protocol approved by the Institutional Care and Use Committee of Baylor College of Medicine (AN-6191). In vivo studies were performed in female and male 8-week-old NOD/Shi-scid/IL-2Rγnull (NOG) mice (Taconic Biosciences, Hudson, NY).

Tissue obtained to create the patient derived xenograft (PDX) model HB17 was performed under the human protocol approved by the Institutional Care and Use Committee of Baylor College of Medicine (H-38834). All patient derived xenograft models in Figure 4D were validated to the patient through single tandem repeat (STR) assays, RNA sequencing, and immunohistochemistry (IHC).

IVIS Imaging. The mice underwent bioluminescence imaging at 24, 48, 72 h in vivo after injection of ICG or I-ICG with the *In Vivo* Imaging System (IVIS, PerkinElmer, Waltham, MA), and luminescence flux was recorded to assess tumor growth. At 72 h the mice were euthanized and imaged ex vivo using the same procedure.

Table S1. Photophysical properties and cLog*P* of ICG compounds in water or 10 mg/mL bovine serum albumin (BSA) in PBS pH 7.2. Excitation = 690 nm, emission = 710–900 nm. λ_{max} (abs) = absorbance wavelength maximum, ε = extinction coefficient, λ_{max} (em) = emission wavelength maximum, and Φ = emission quantum yield.

Compound	λ_{max} (abs), nm (ε, $M^{-1}cm^{-1}$) water	λ_{max} (abs), nm (ε, $M^{-1}cm^{-1}$) BSA/PBS	λ_{max} (em), nm (Φ, %) water	λ_{max} (em), nm (Φ, %) BSA/PBS	cLog*P*[a]
ICG	780 (126000 ± 7000)	794 (136000 ± 15000)	806 (2.3)	800 (4.6)	-3.41
4-mono-I-ICG	761 (153000 ± 20000)	782 (81000 ± 21000)	784 (2.8)	790 (3.4)	-3.46
4-I-ICG	745 (151000 ± 32000)	765 (73000 ± 21000)	770 (12.3)	774 (4.3)	-3.51
5-I-ICG	756 (103000 ± 4000)	765 (64000 ± 6000)	781 (6.4)	778 (7.8)	-3.51
6-I-ICG	746 (96000 ± 17000)	753 (65000 ± 12000)	772 (9.7)	772 (10.5)	-3.51

[a]cLog*P* determined using ChemDraw 19.1

Table S2. The top putative ICG transporters as identified through next-generation sequencing (NGS) from the SLC-CRISPRa screen.

#	Gene	Count	%	Name	Type	Substrate	Tissue and cellular expression
1	SLC25A15	78438	30.9	ORC1, ORNT1, SP1855	Exchanger	ornithine, citrulline, lysine, arginine (H^+)	liver, pancreas, lung, testes, small intestine, spleen, kidneys, brain, heart,

							inner mitochondrial membrane
2	SLCO1B3	36348	14.3	OATP1B3	–	bile salts, organic anions	liver (hepatocytes)
3	SLC8B1	31887	12.6	NCLX	Exchanger	Na^+, Li^+, Ca^{2+}	mitochondria of mammalian skeletal and heart muscle, neurons, β-cells, B-cells, liver contains relatively small amounts
4	SLC4A11	29834	11.8	BTR1	Co-transporter	sodium, borate	kidneys, salivary gland, testes, thyroid, trachea
5	SLC5A12	29703	11.7	SMCT2	Co-transporter	short chain fatty acids (Na^+)	intestine, brain, retina, muscle
6	SLC35B1	15616	6.2	UGTREL1	–	–	ubiquitous in tissues, endoplasmic reticulum membrane

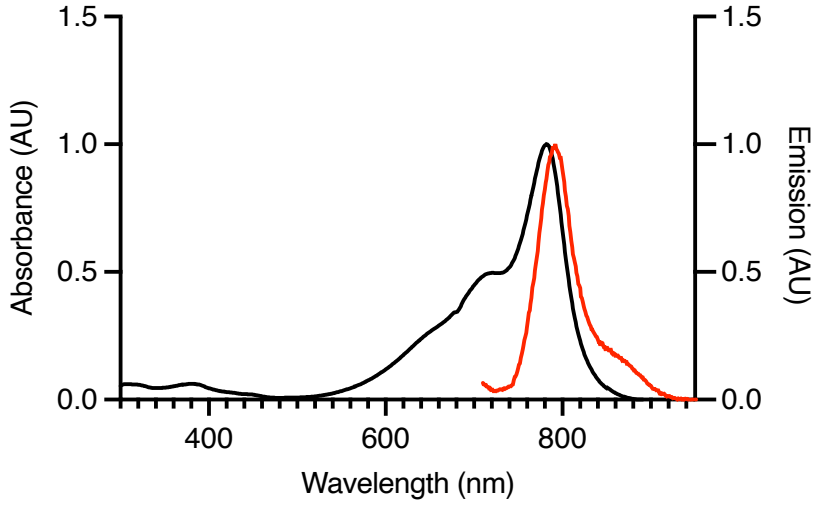

Figure S1. Absorbance (black trace) and emission (red trace) of **4-mono-I-ICG** in 10 mg/mL BSA/PBS.

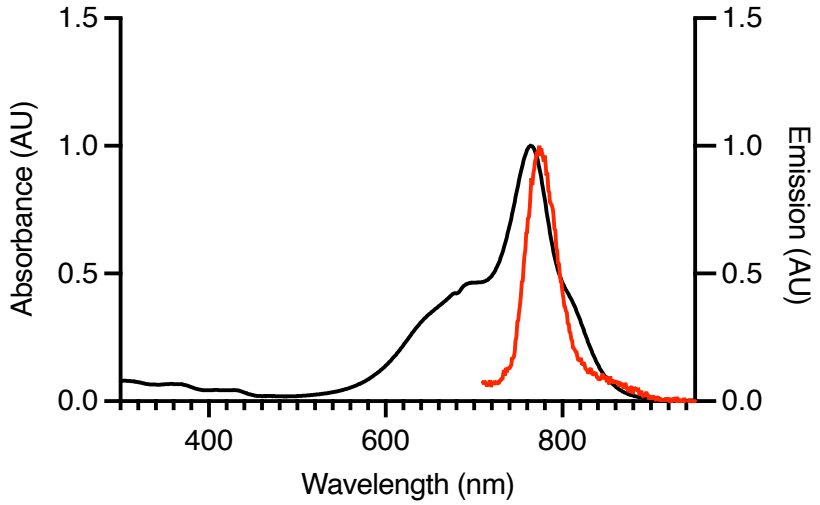

Figure S2. Absorbance (black trace) and emission (red trace) of **4-I-ICG** in 10 mg/mL BSA/PBS.

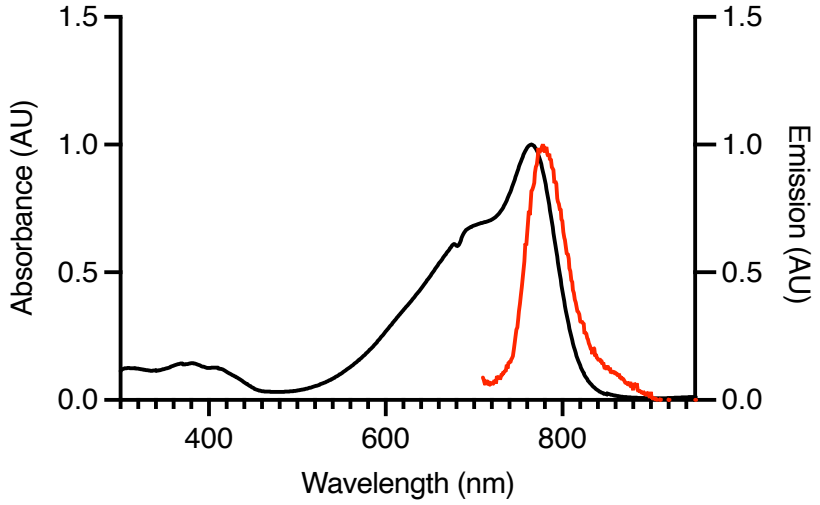

Figure S3. Absorbance (black trace) and emission (red trace) of **5-I-ICG** in 10 mg/mL BSA/PBS.

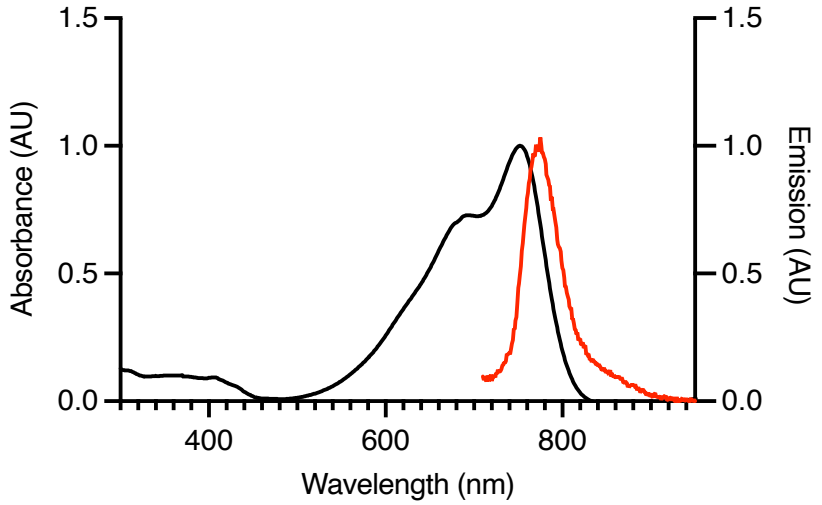

Figure S4. Absorbance (black trace) and emission (red trace) of **6-I-ICG** in 10 mg/mL BSA/PBS.

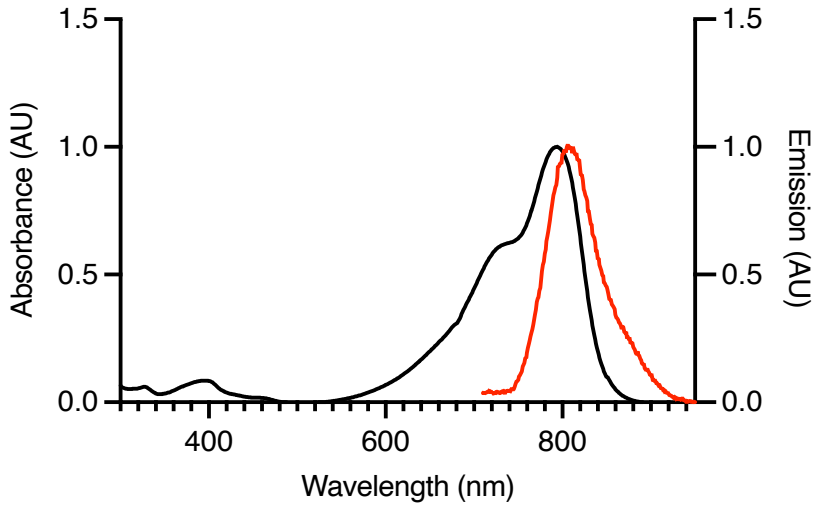

Figure S5. Absorbance (black trace) and emission (red trace) of **ICG** in 10 mg/mL BSA/PBS.

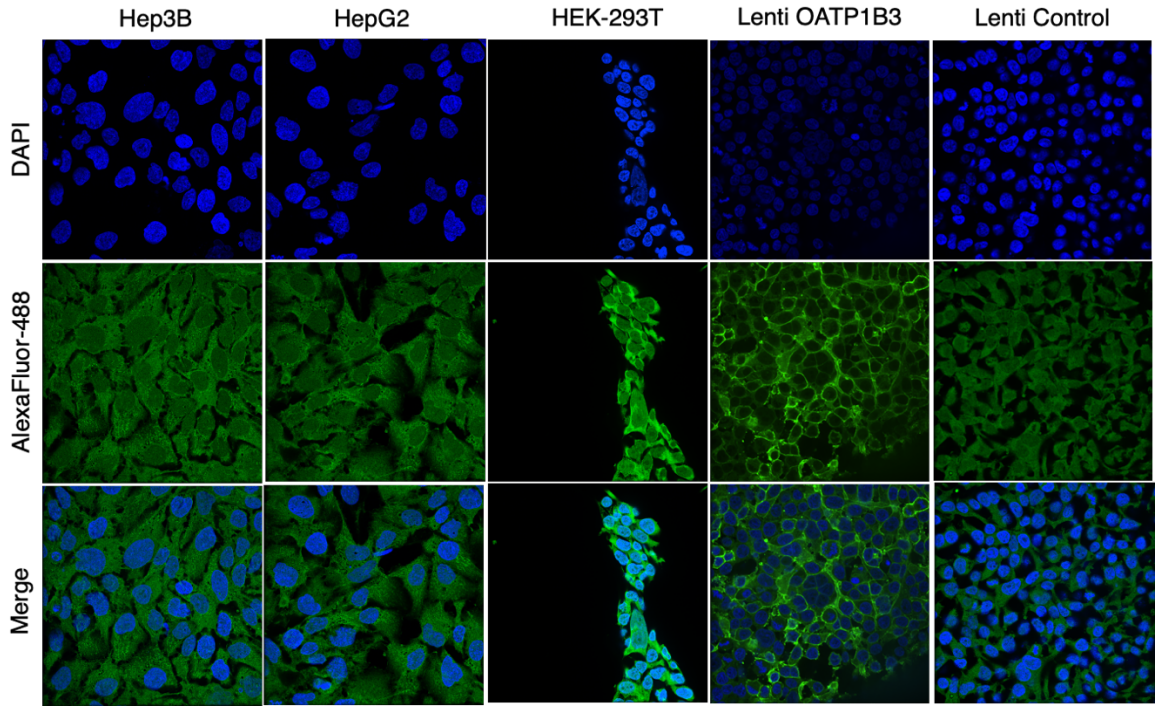

Figure S6. Confocal fluorescence microscope images of cells incubated with a primary anti-OATP1B3 antibody overnight (4°C), then for 1 h with an AlexaFluor-488-goat-anti-mouse IgG (H+L) at room temperature. Cells were stained with DAPI and imaged in Hank's Buffered Saline Solution (HBSS) with a 63x oil immersed lens.

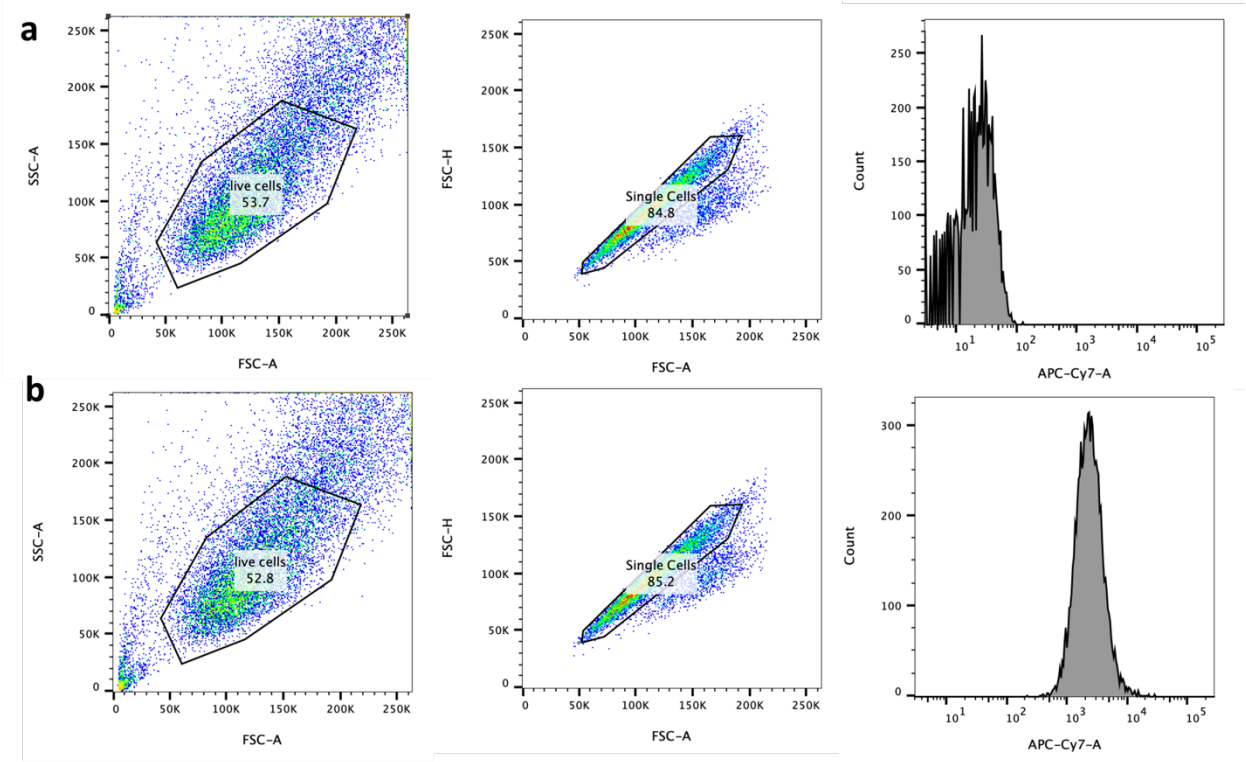

Figure S7. Flow cytometry analysis of **a. blank** and **b. ICG** (10 μM) in Hep3B cells after 1 h incubation. A representative FlowJo analysis of the study provides gating used for live cells, single cells, and histogram in APC-Cy7 channel.

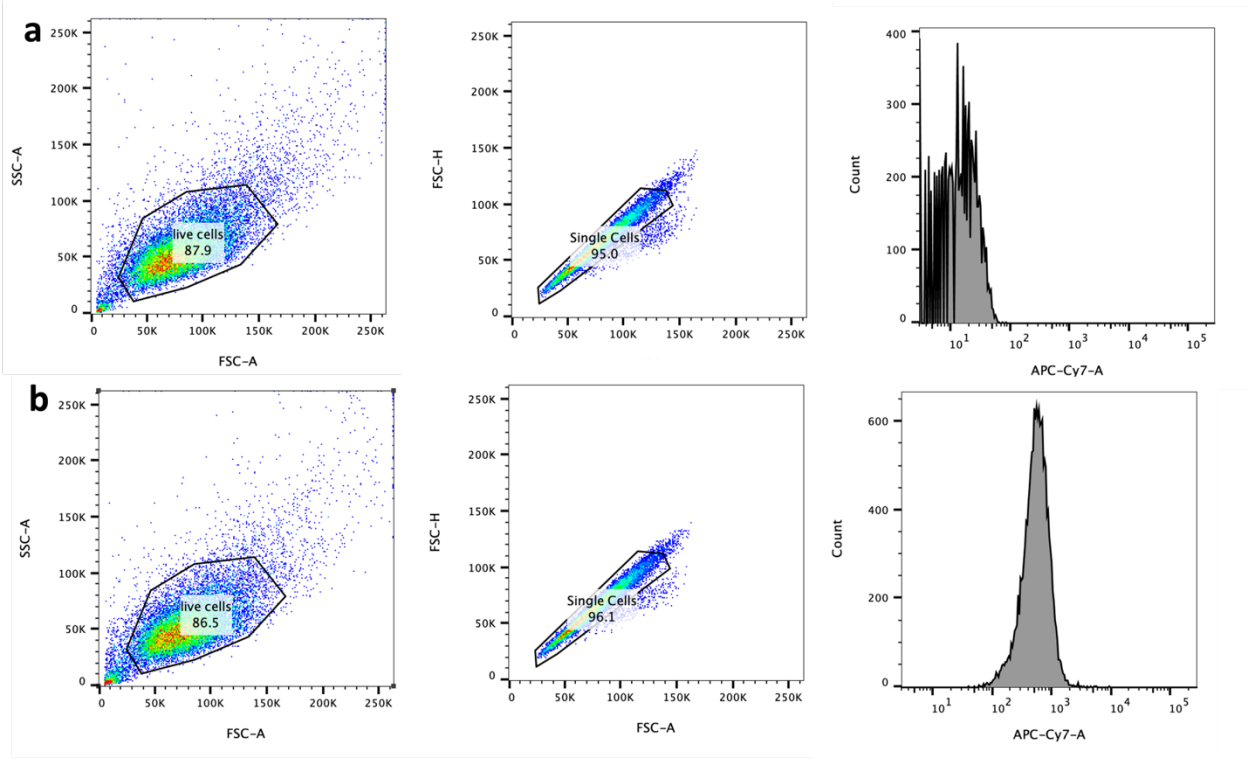

Figure S8. Flow cytometry analysis of **a. blank** and **b. ICG** (10 μM) in HEK-293T cells after 1 h incubation. A representative FlowJo analysis of the study provides gating used for live cells, single cells, and histogram in APC-Cy7 channel.

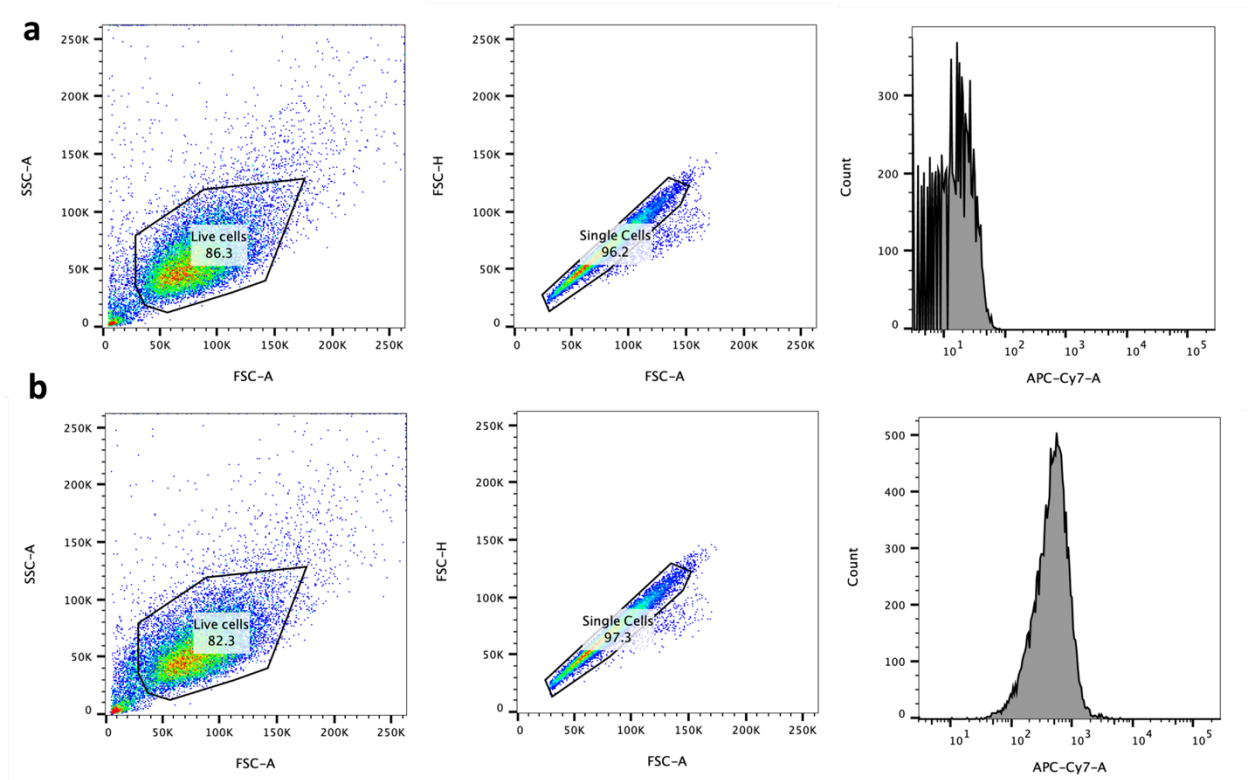

Figure S9. Flow cytometry analysis of **a. blank** and **b. ICG** (10 μM) in OATP1c1.v1 HEK-293T (MOI 10) cells after 1 h incubation. A representative FlowJo analysis of the study provides gating used for live cells, single cells, and histogram in APC-Cy7 channel.

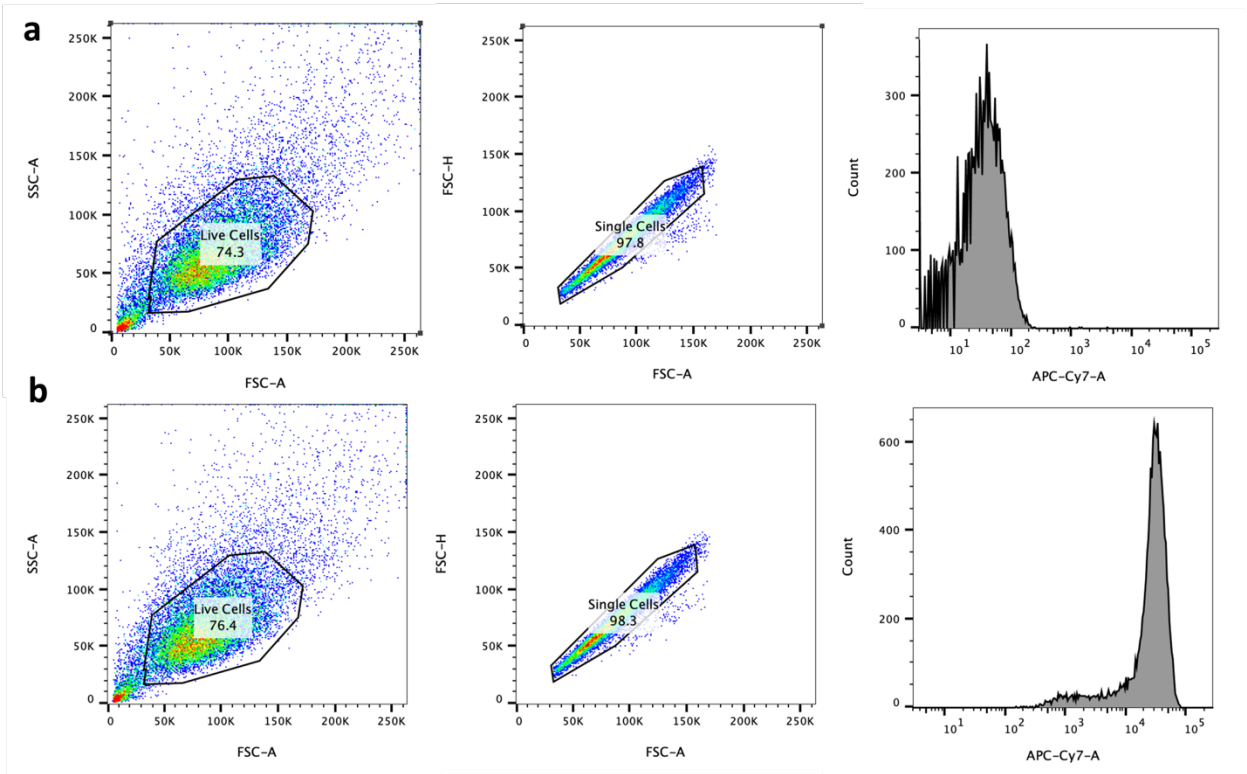

Figure S10. Flow cytometry analysis of **a. blank** and **b. ICG** (10 μM) in OATP1B3 HEK-293T (Lenti OATP1B3, MOI 10) cells after 1 h incubation. A representative FlowJo analysis of the study provides gating used for live cells, single cells, and histogram in APC-Cy7 channel.

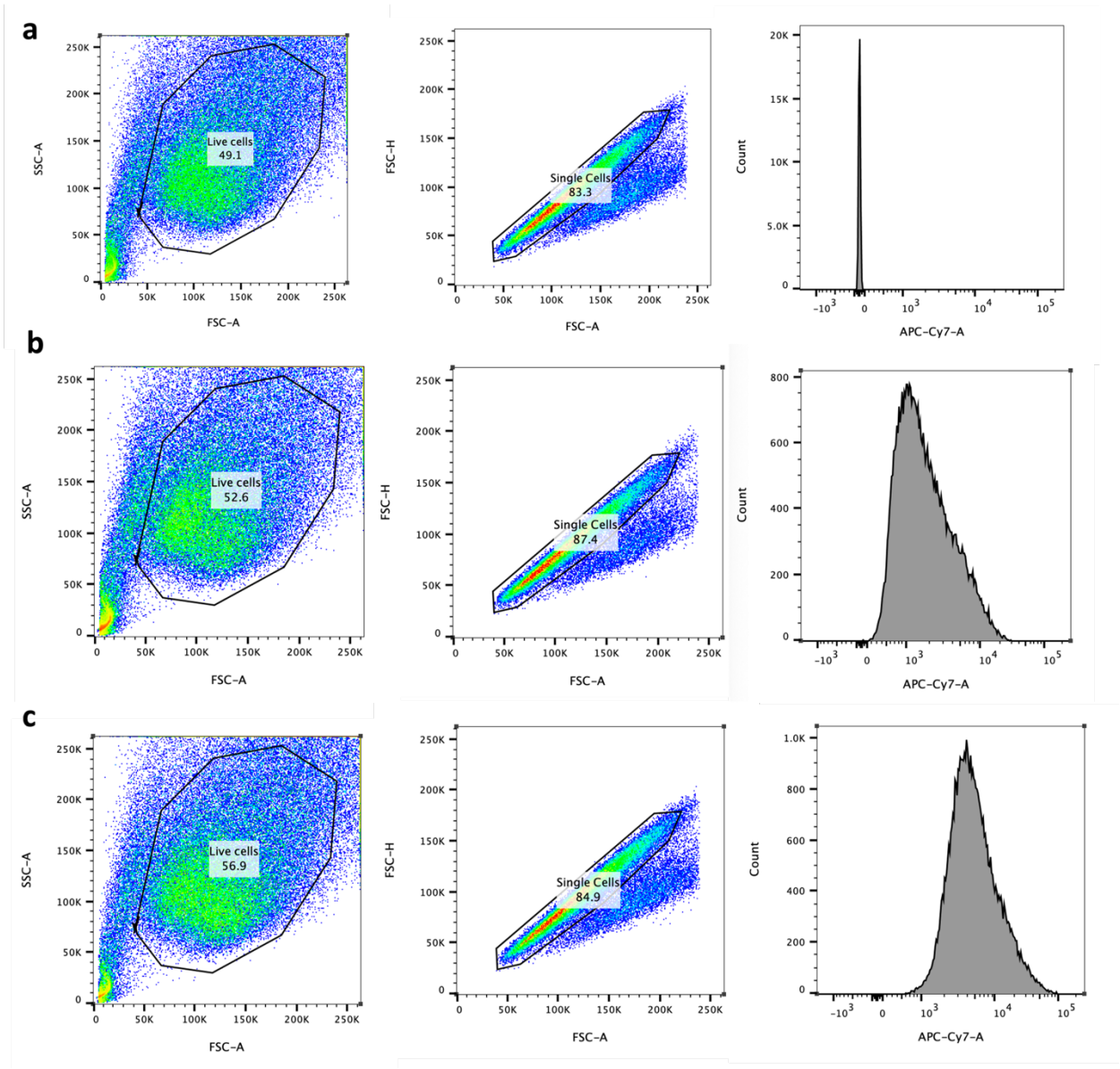
a
SSC-A
FSC-A
Live cells
49.1
FSC-H
FSC-A
Single Cells
83.3
Count
APC-Cy7-A
b
SSC-A
FSC-A
Live cells
52.6
FSC-H
FSC-A
Single Cells
87.4
Count
APC-Cy7-A
c
SSC-A
FSC-A
Live cells
56.9
FSC-H
FSC-A
Single Cells
84.9
Count
APC-Cy7-A

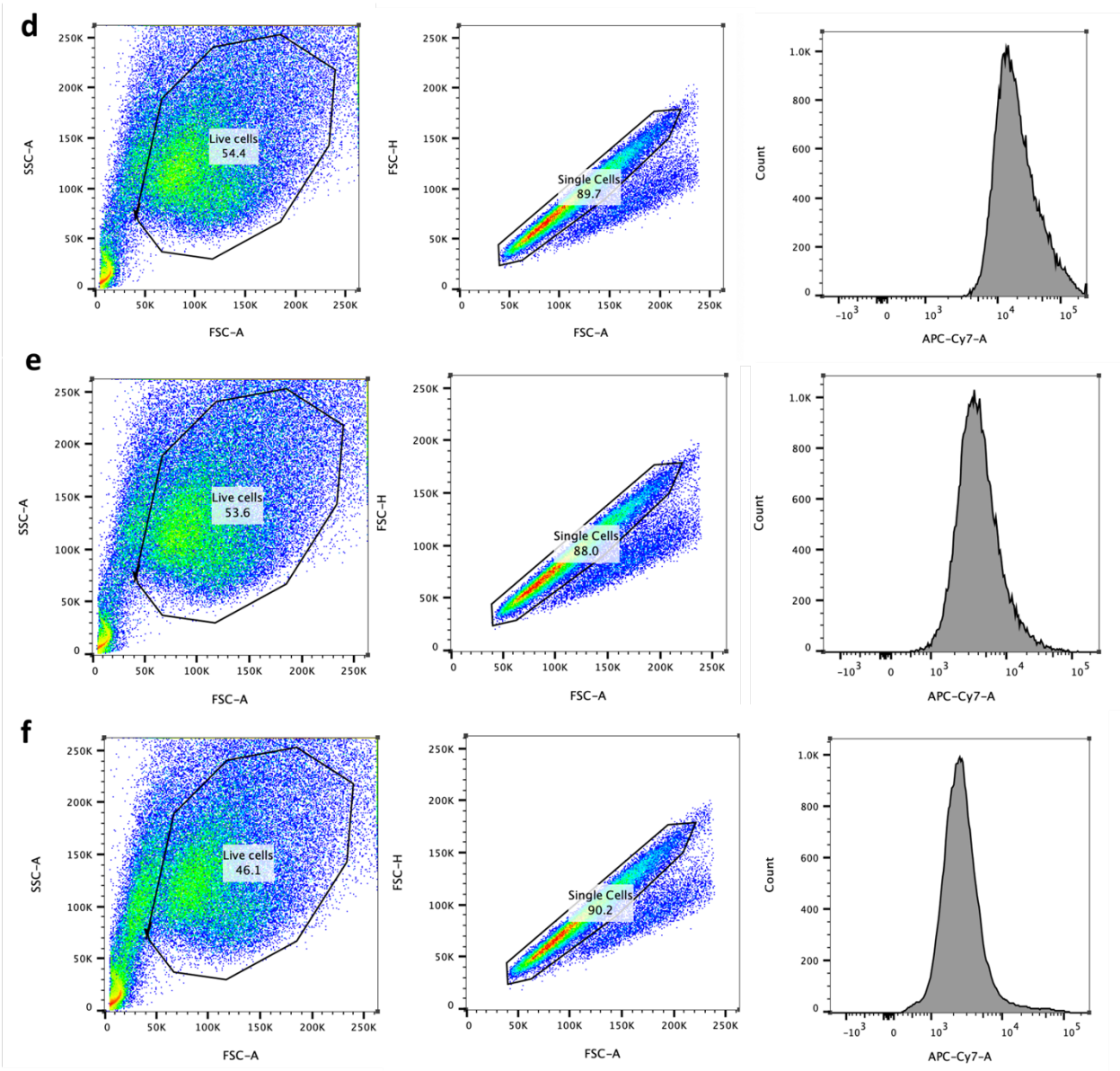

Figure S11. Flow cytometry analysis of **a. blank**, **b. ICG**, **c. 4-mono-I-ICG**, **d. 4-I-ICG**, **e. 5-I-ICG**, and **f. 6-I-ICG** (10 μM) in HepG2 cells after 1 h incubation. A representative FlowJo analysis of the study provides gating used for live cells, single cells, and histogram in APC-Cy7 channel.

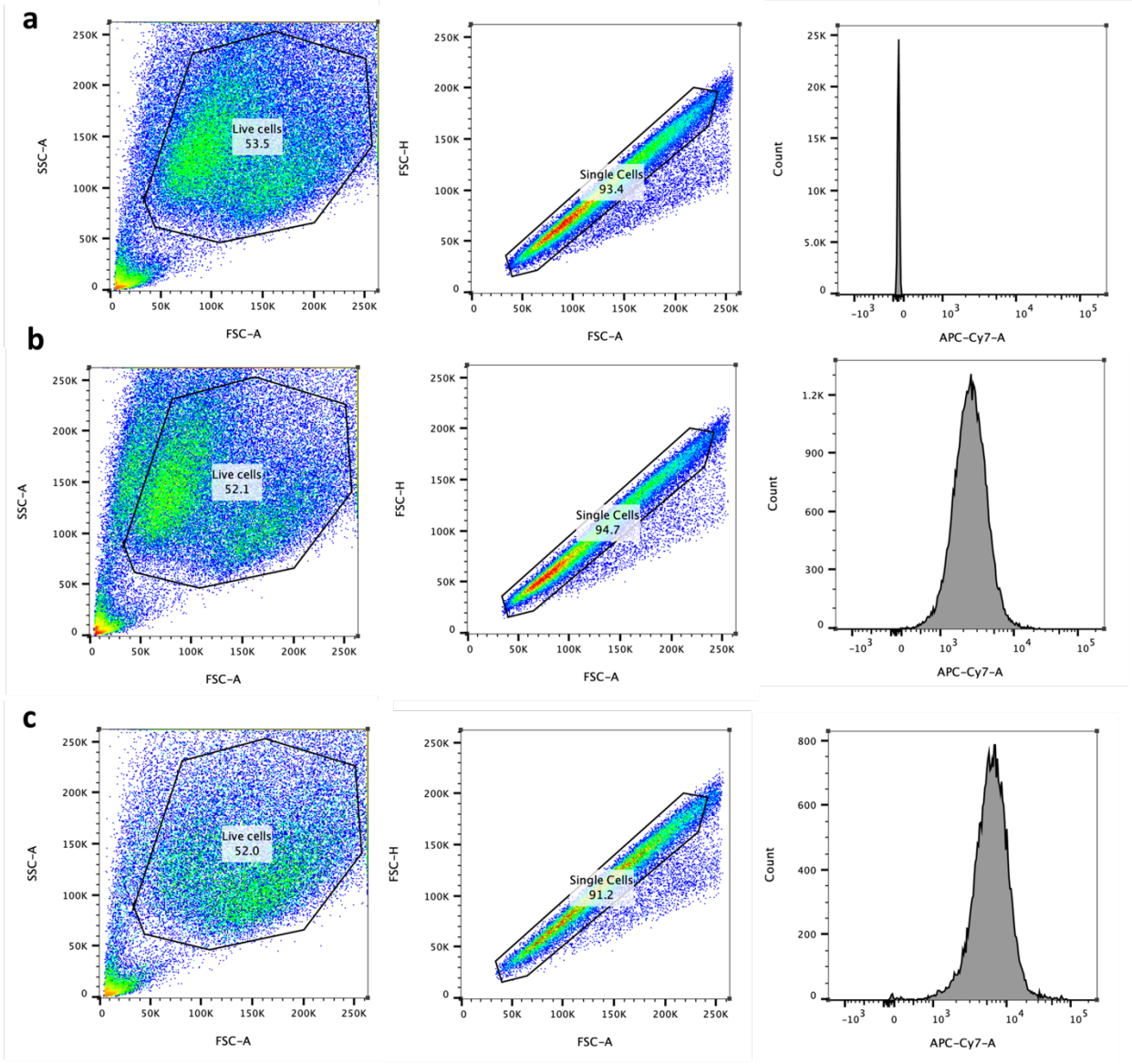
a
SSC-A
FSC-A
Live cells
53.5
FSC-H
Single Cells
93.4
Count
APC-Cy7-A
b
Live cells
52.1
Single Cells
94.7
c
Live cells
52.0
Single Cells
91.2

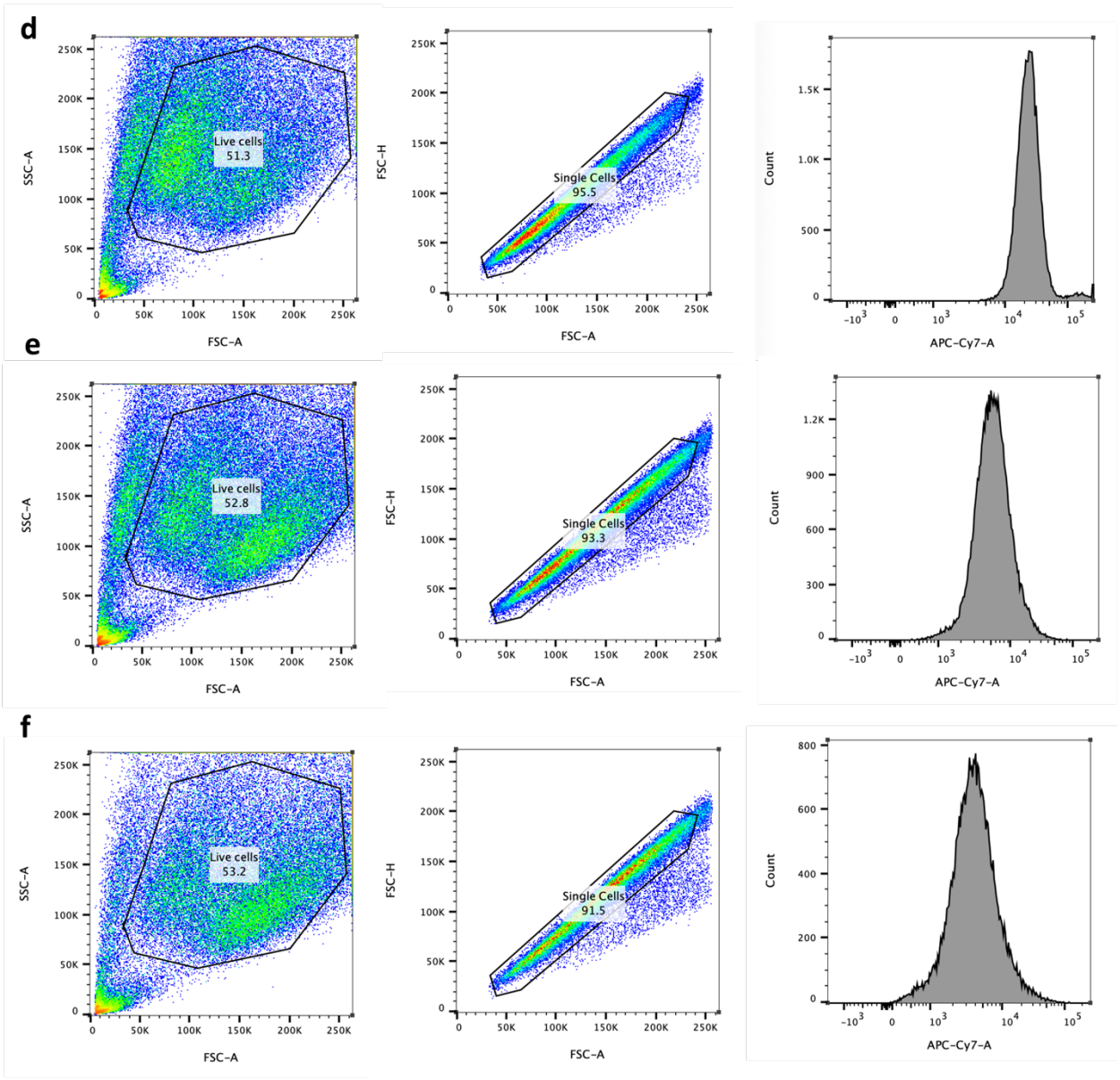

Figure S12. Flow cytometry analysis of **a. blank**, **b. ICG**, **c. 4-mono-I-ICG**, **d. 4-I-ICG**, **e. 5-I-ICG**, and **f. 6-I-ICG** (10 μM) in Hep3B cells after 1 h incubation. A representative FlowJo analysis of the study provides gating used for live cells, single cells, and histogram in APC-Cy7 channel.

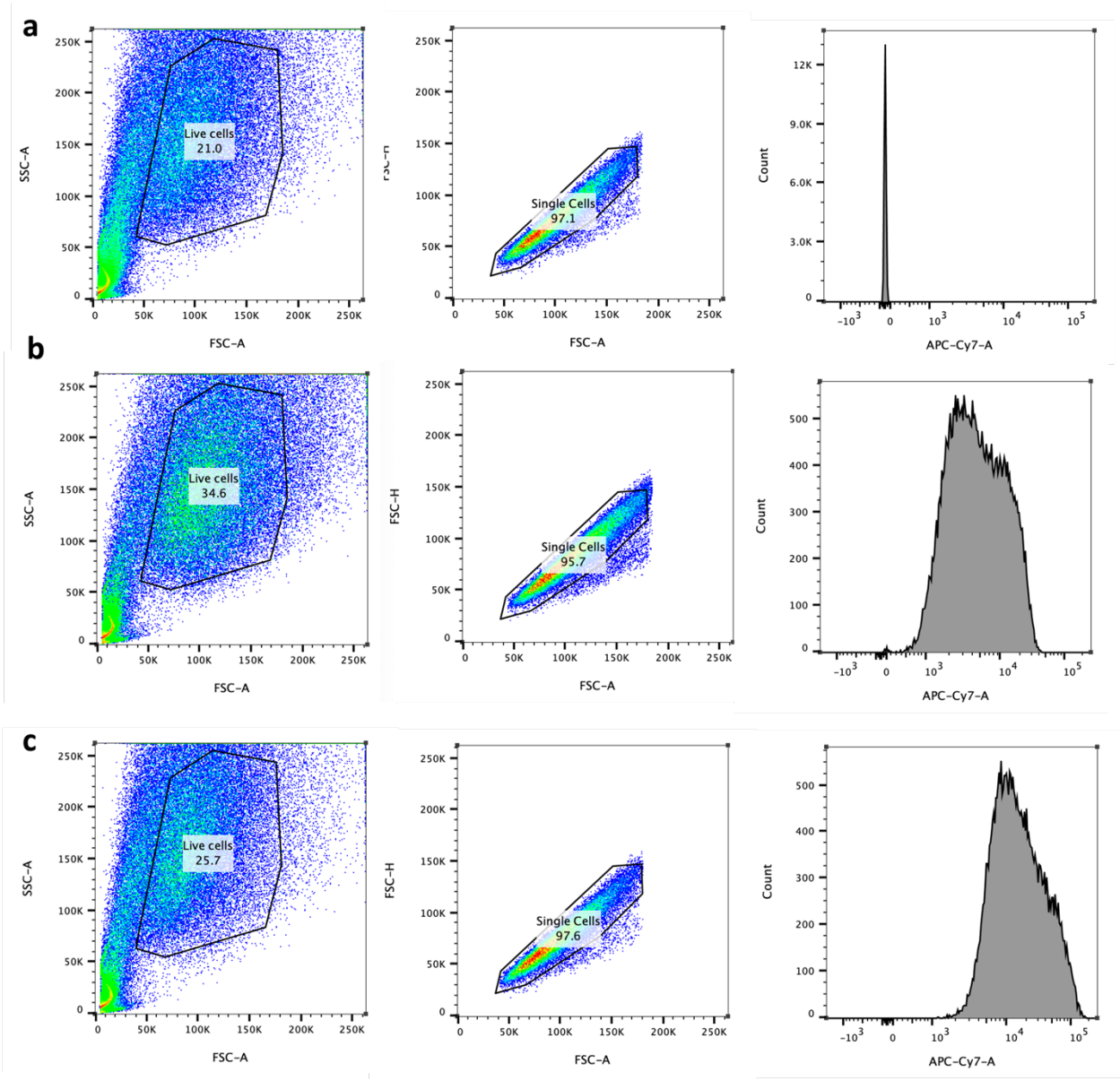
a
SSC-A
FSC-A
Live cells
21.0
FSC-H
Single Cells
97.1
Count
APC-Cy7-A
b
SSC-A
FSC-A
Live cells
34.6
FSC-H
Single Cells
95.7
Count
APC-Cy7-A
c
SSC-A
FSC-A
Live cells
25.7
FSC-H
Single Cells
97.6
Count
APC-Cy7-A

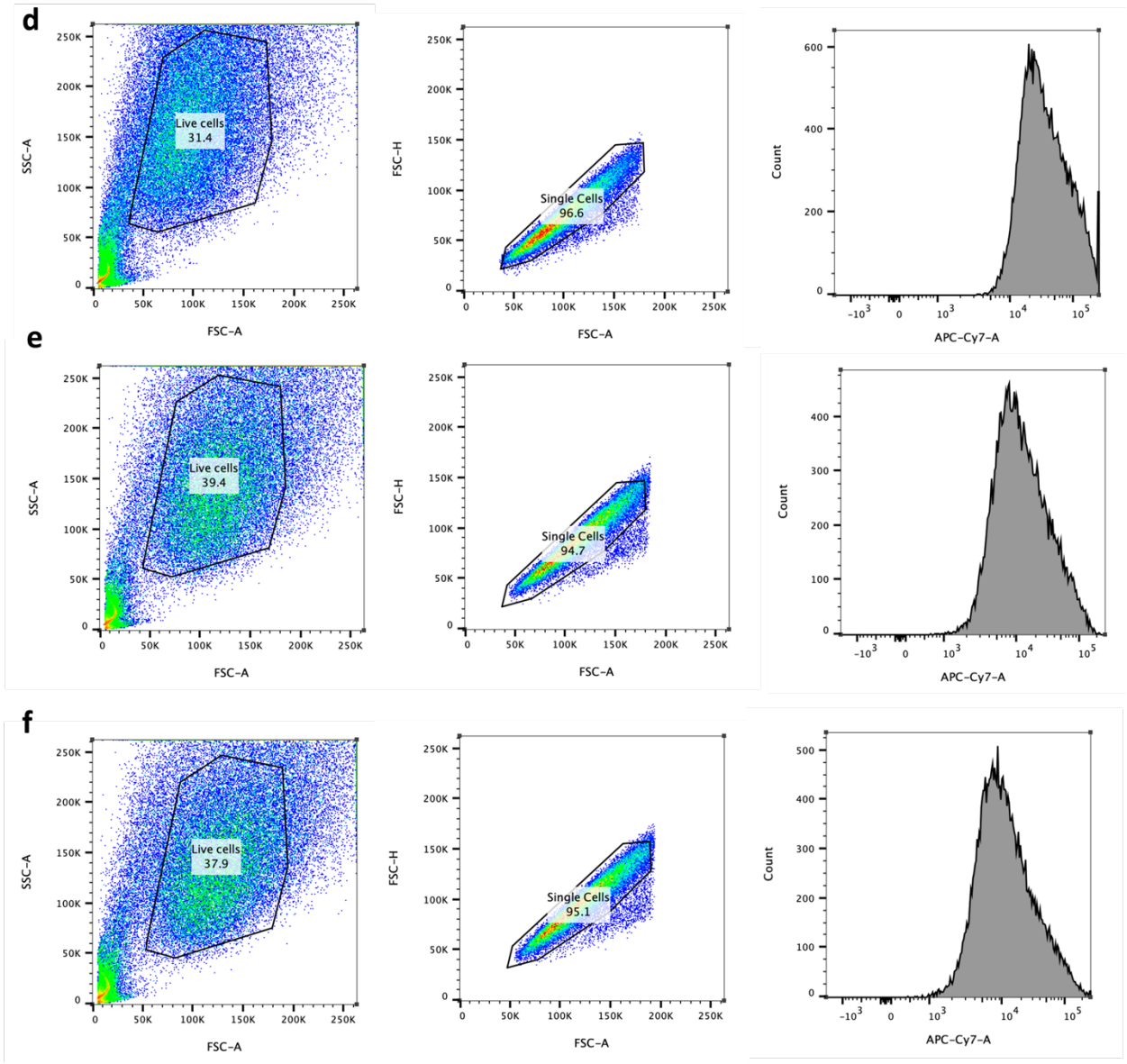

Figure S13. Flow cytometry analysis of **a. blank**, **b. ICG**, **c. 4-mono-I-ICG**, **d. 4-I-ICG**, **e. 5-I-ICG**, and **f. 6-I-ICG** (10 μM) in Huh-7 cells after 1 h incubation. A representative FlowJo analysis of the study provides gating used for live cells, single cells, and histogram in APC-Cy7 channel.

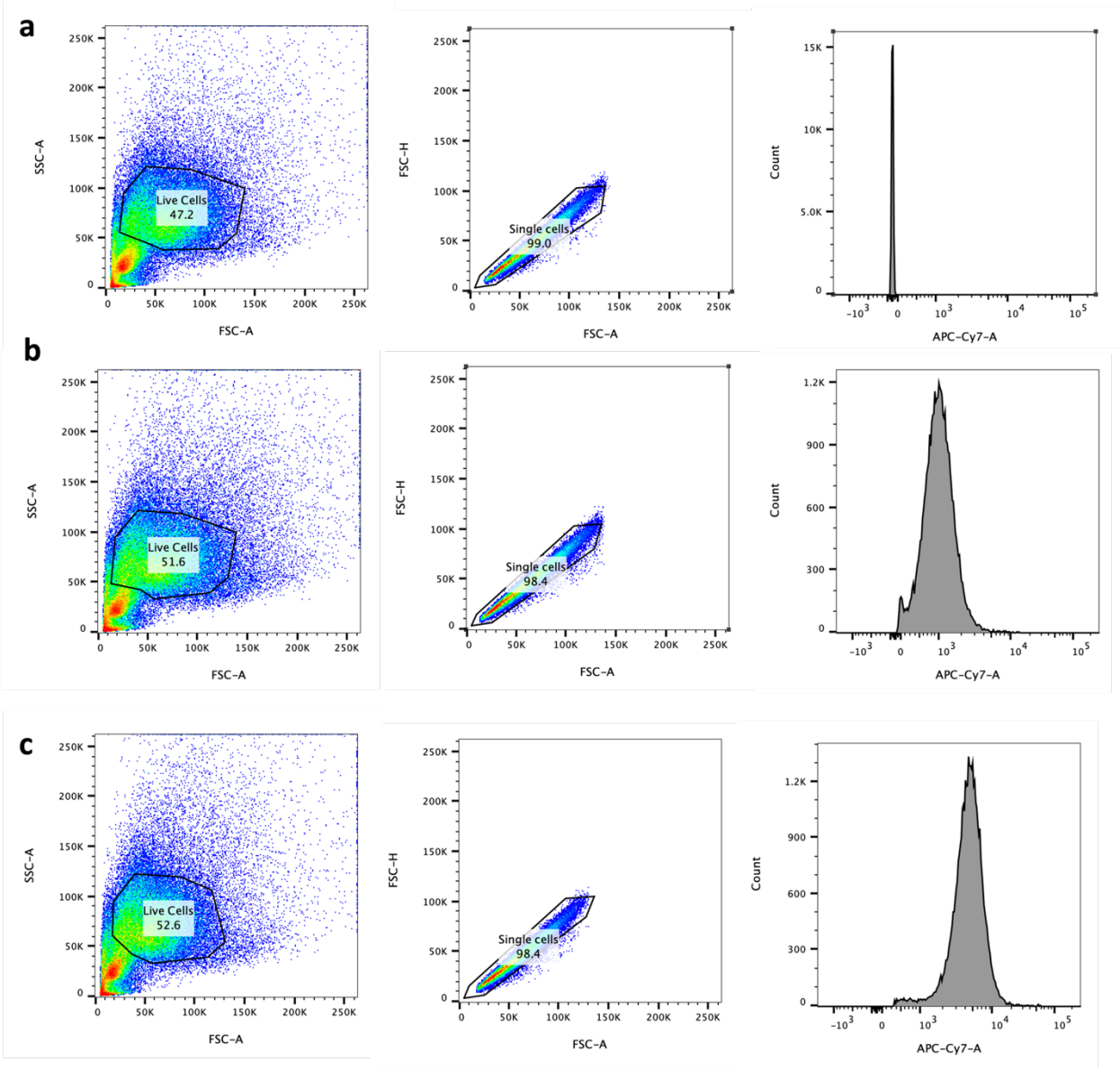
a
SSC-A
FSC-A
Live Cells
47.2
FSC-H
FSC-A
Single cells
99.0
Count
APC-Cy7-A
b
SSC-A
FSC-A
Live Cells
51.6
FSC-H
FSC-A
Single cells
98.4
Count
APC-Cy7-A
c
SSC-A
FSC-A
Live Cells
52.6
FSC-H
FSC-A
Single cells
98.4
Count
APC-Cy7-A

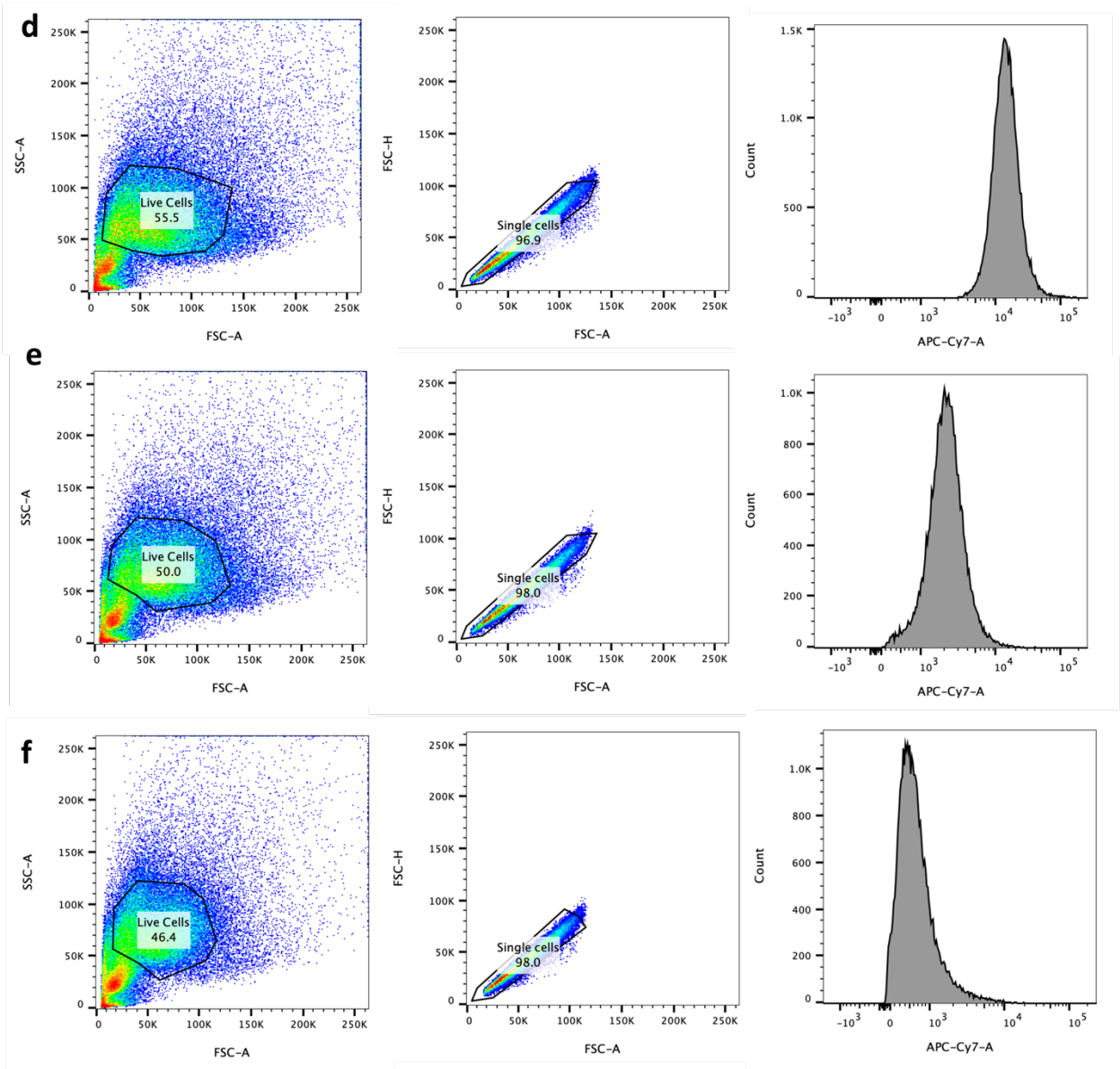

Figure S14. Flow cytometry analysis of **a. blank**, **b. ICG**, **c. 4-mono-I-ICG**, **d. 4-I-ICG**, **e. 5-I-ICG**, and **f. 6-I-ICG** (10 μM) in HEK-293T cells after 1 h incubation. A representative FlowJo analysis of the study provides gating used for live cells, single cells, and histogram in APC-Cy7 channel.

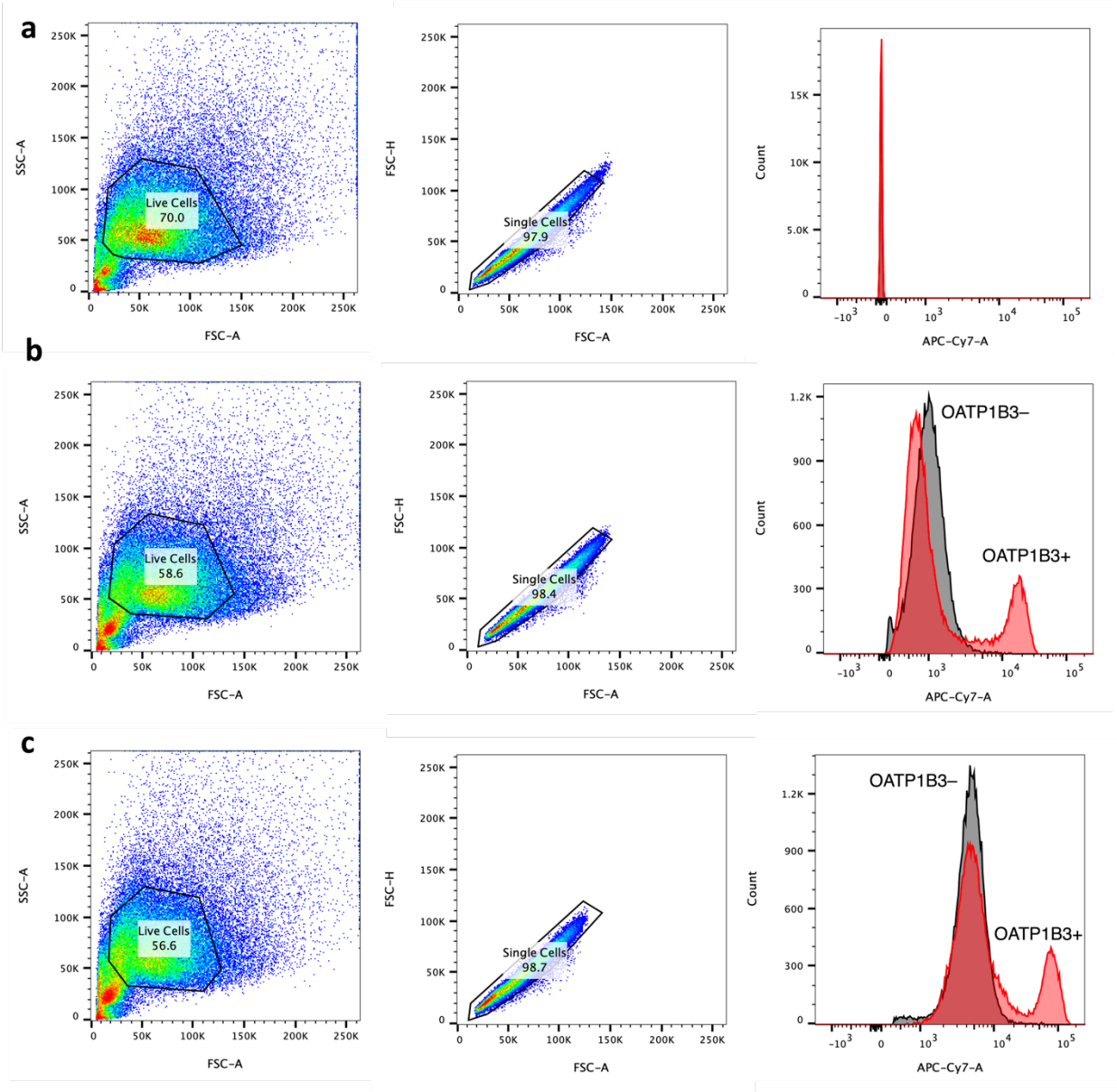
a
SSC-A
FSC-A
Live Cells
70.0
FSC-H
FSC-A
Single Cells
97.9
Count
APC-Cy7-A
b
SSC-A
FSC-A
Live Cells
58.6
FSC-H
FSC-A
Single Cells
98.4
Count
OATP1B3–
OATP1B3+
APC-Cy7-A
c
SSC-A
FSC-A
Live Cells
56.6
FSC-H
FSC-A
Single Cells
98.7
Count
OATP1B3–
OATP1B3+
APC-Cy7-A

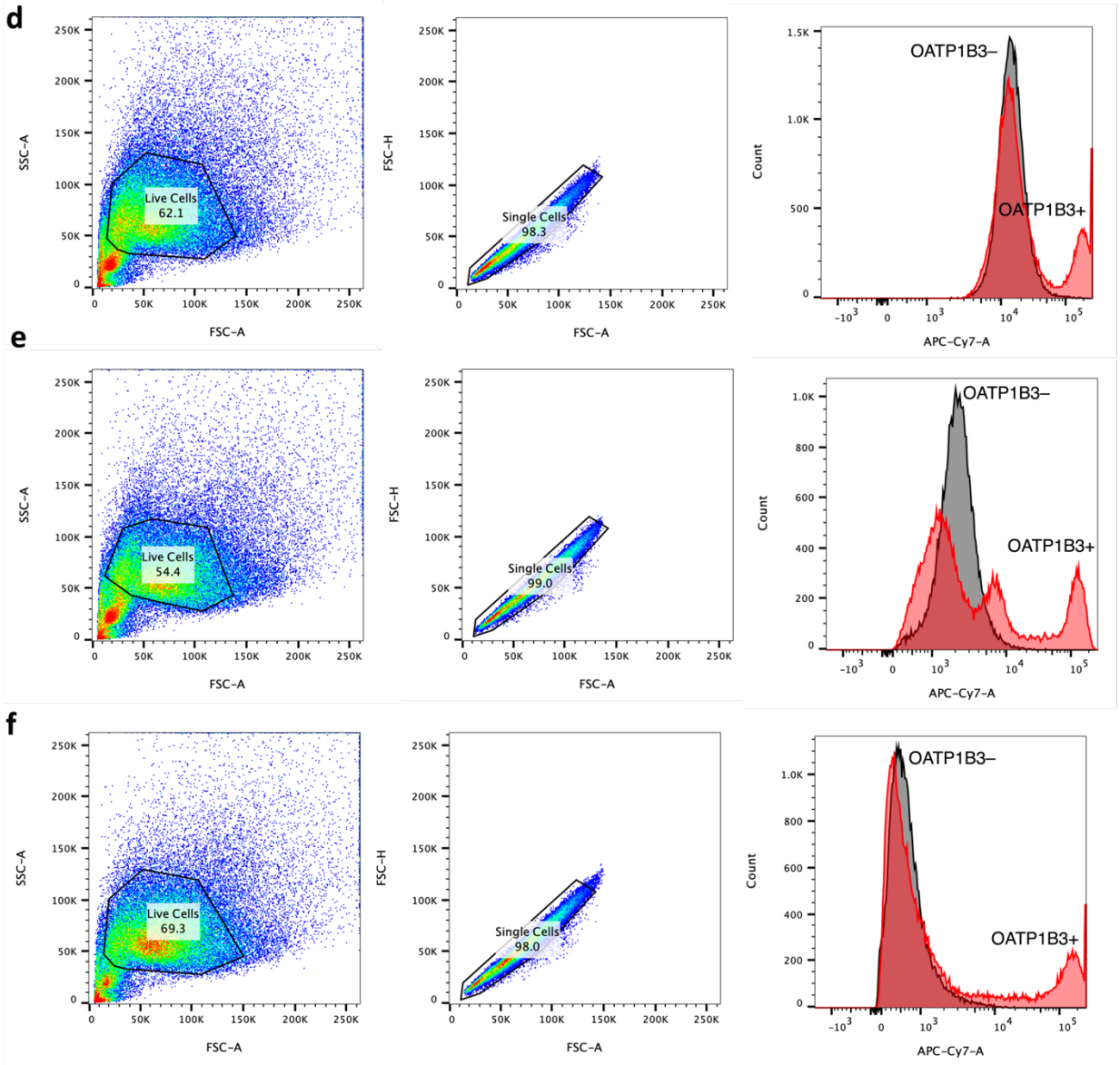

Figure S15. Flow cytometry analysis of **a. blank**, **b. ICG**, **c. 4-mono-I-ICG**, **d. 4-I-ICG**, **e. 5-I-ICG**, and **f. 6-I-ICG** (10 μM) in OATP1B3 HEK-293T (MOI 10) cells after 1 h incubation. Two separate cell populations were observed. These populations correspond to OATP1B3+ and OATP1B3– cells, which indicates that the transfection is not stable over time. Cells were gated using only the OATP1B3+ population. Red traces indicate OATP1B3 HEK-293T (MOI 10) cells and black traces show HEK-293T cells. A representative FlowJo analysis of the study provides gating used for live cells, single cells, and histogram in APC-Cy7 channel.

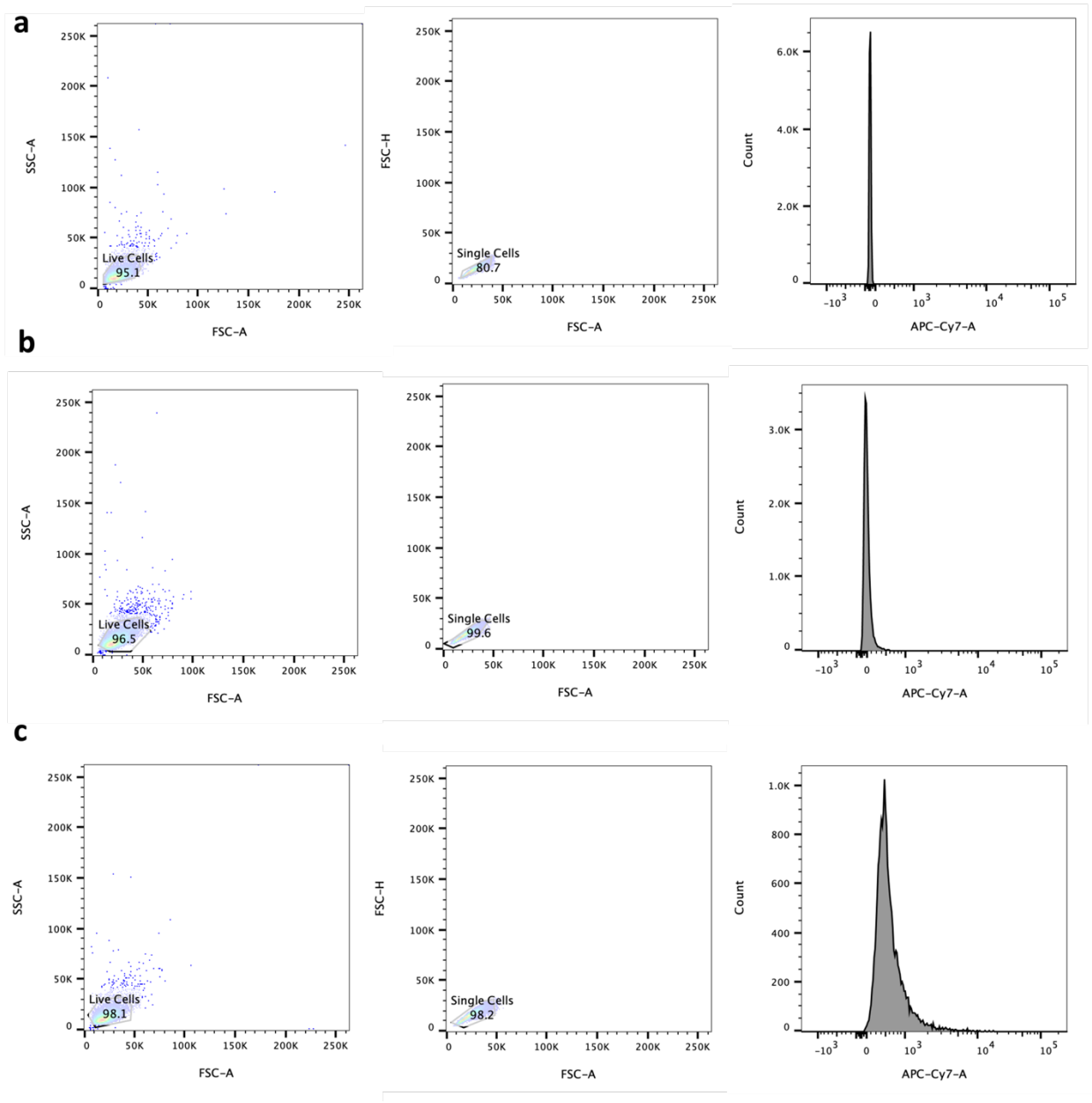

Figure S16. Flow cytometry analysis of **a. blank**, **b. ICG**, and **c. 4-mono-I-ICG**, (25 μM) in SH-SY5Y cells after 1 h incubation. A representative FlowJo analysis of the study provides gating used for live cells, single cells, and histogram in APC-Cy7 channel.

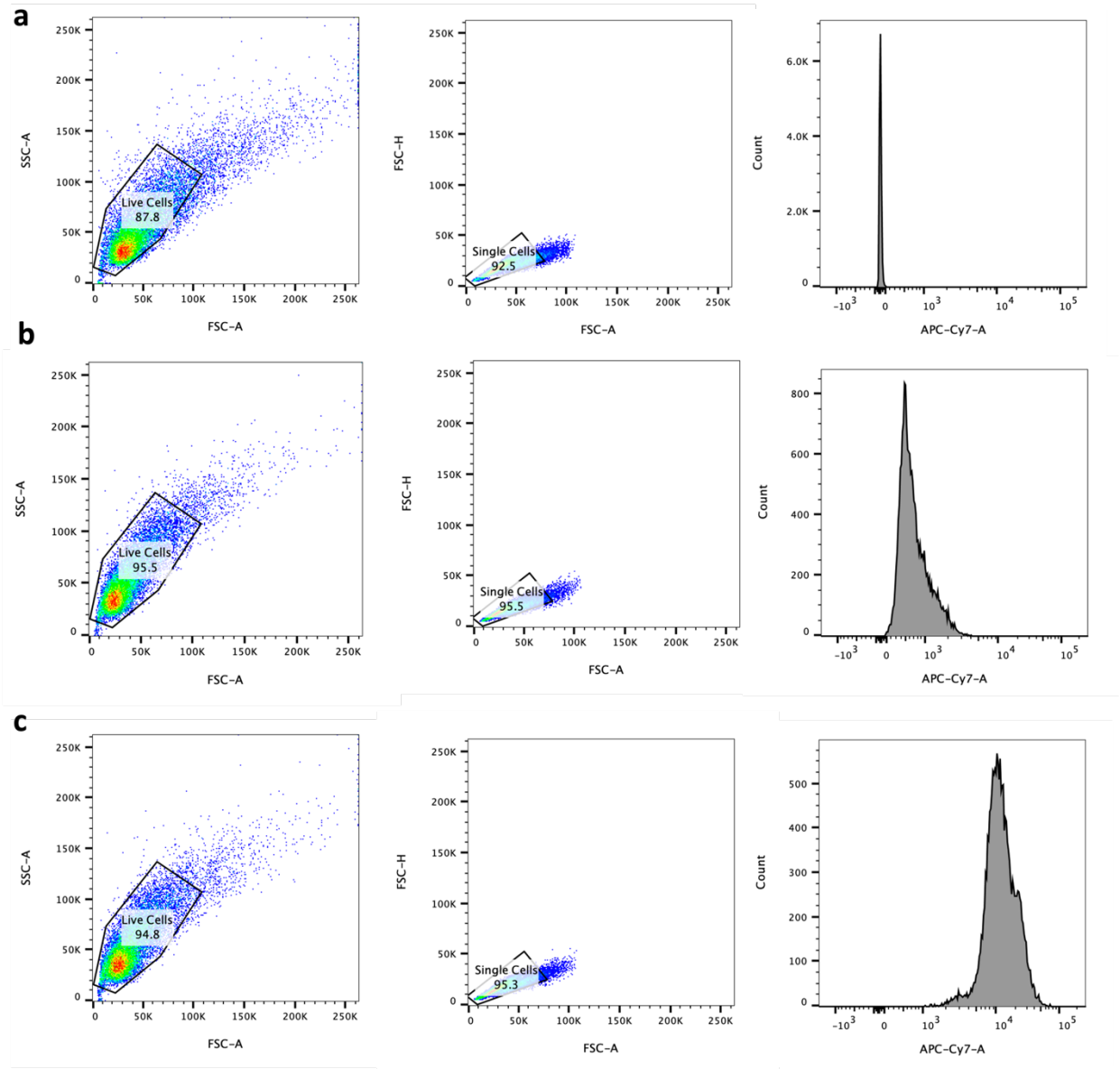

Figure S17. Flow cytometry analysis of **a. blank**, **b. ICG**, and **c. 4-mono-I-ICG**, (25 μM) in HepG2 cells after 1 h incubation. A representative FlowJo analysis of the study provides gating used for live cells, single cells, and histogram in APC-Cy7 channel.

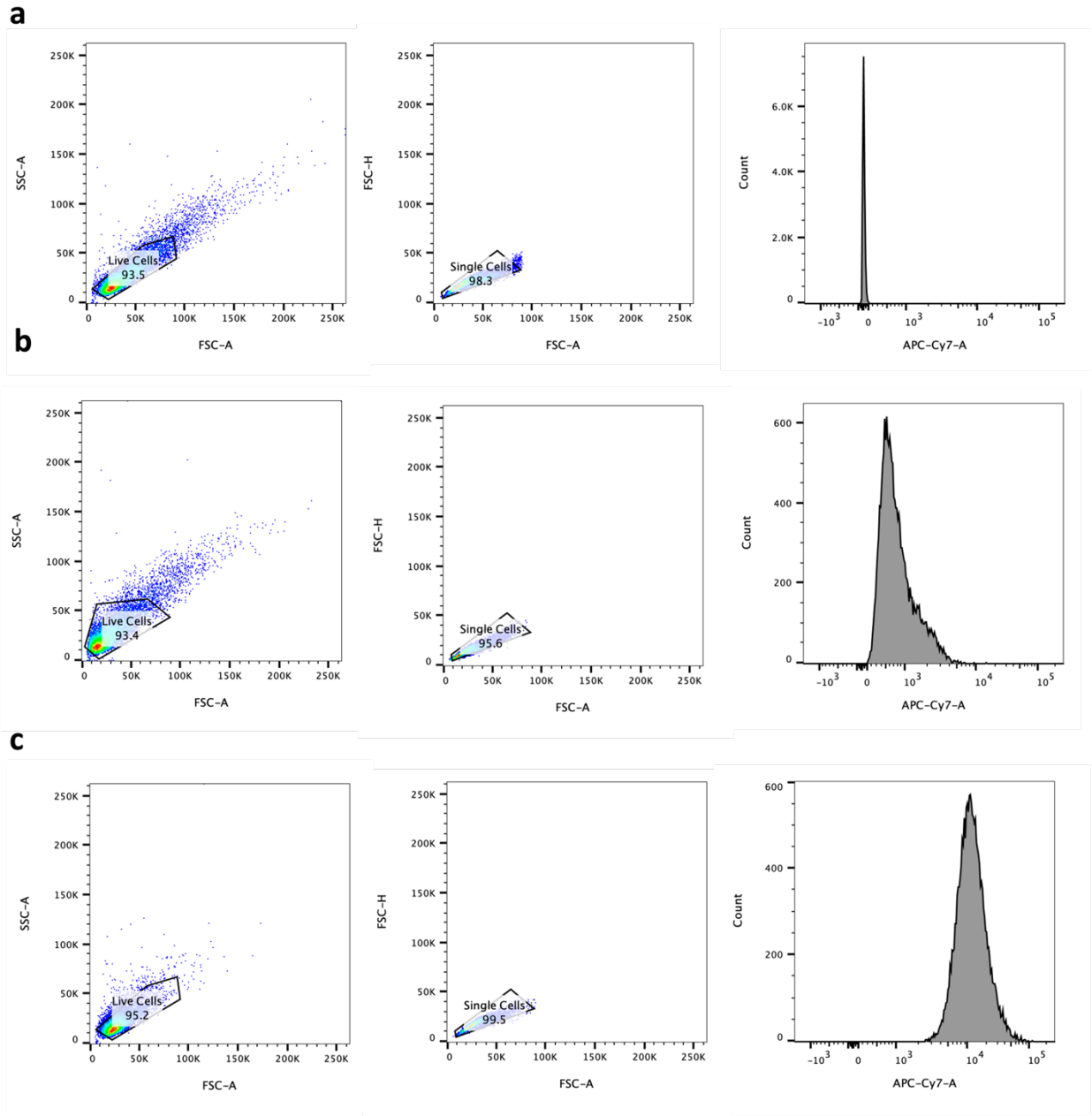

Figure S18. Flow cytometry analysis of **a. blank**, **b. ICG**, and **c. 4-mono-I-ICG**, (25 μM) in HB17 cells after 1 h incubation. A representative FlowJo analysis of the study provides gating used for live cells, single cells, and histogram in APC-Cy7 channel.

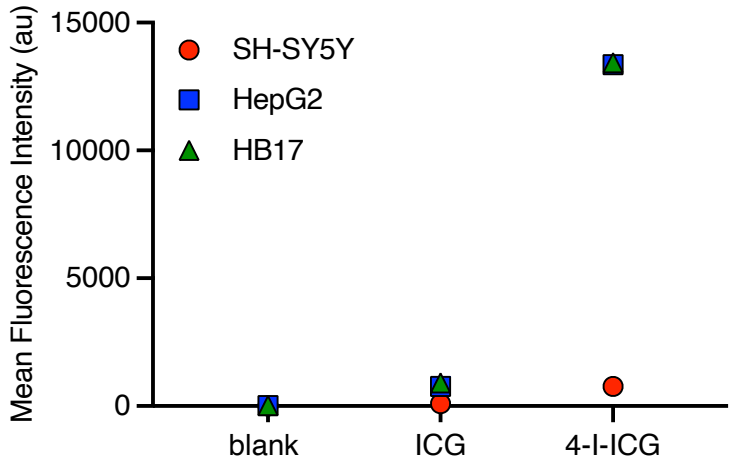

Figure S19. Flow cytometry results showing mean fluorescence intensity of SH-SY5Y, HepG2, and HB17 cells unstained (blank) or stained with **ICG** (25 μM) or **4-I-ICG** (25 μM).

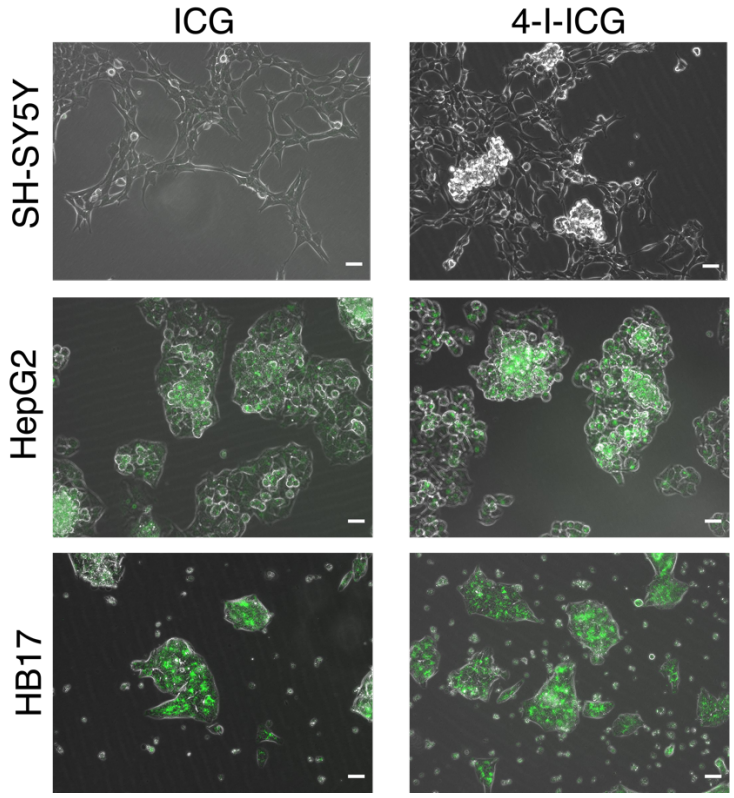

Figure S20. Confocal fluorescence microscopy images of SH-SY5Y, HepG2, or HB17 cells treated with 10 μM of ICG or 4-I-ICG for 1 h. Scale bar = 500 μm.

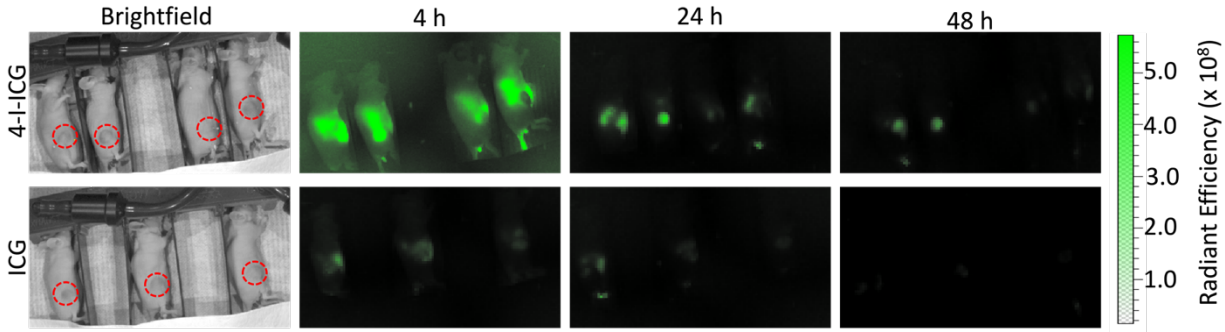

Figure S21. Side view of Hep3B tumor-bearing athymic nude mice treated with **4-I-ICG** (2 mg/kg) and **ICG** (2 mg/kg). Tumors are highlighted in red circles.

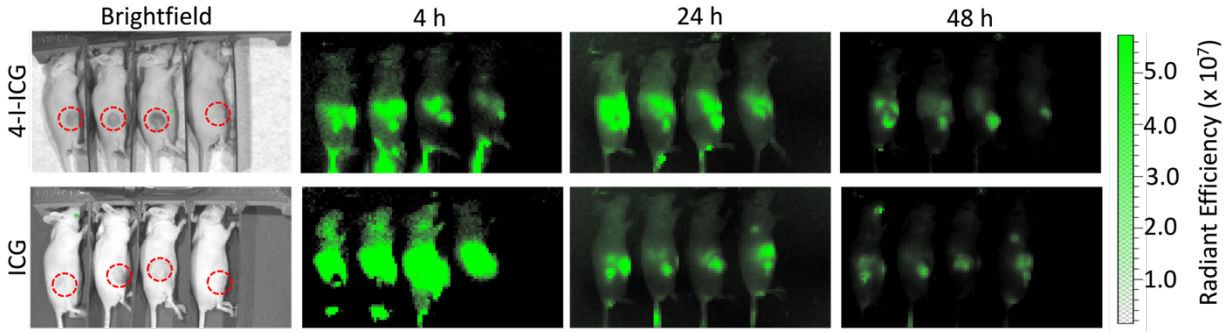

Figure S22. Side view of Huh-7 tumor-bearing athymic nude mice treated with **4-I-ICG** (2 mg/kg) and **ICG** (2 mg/kg). Tumors are highlighted in red circles.

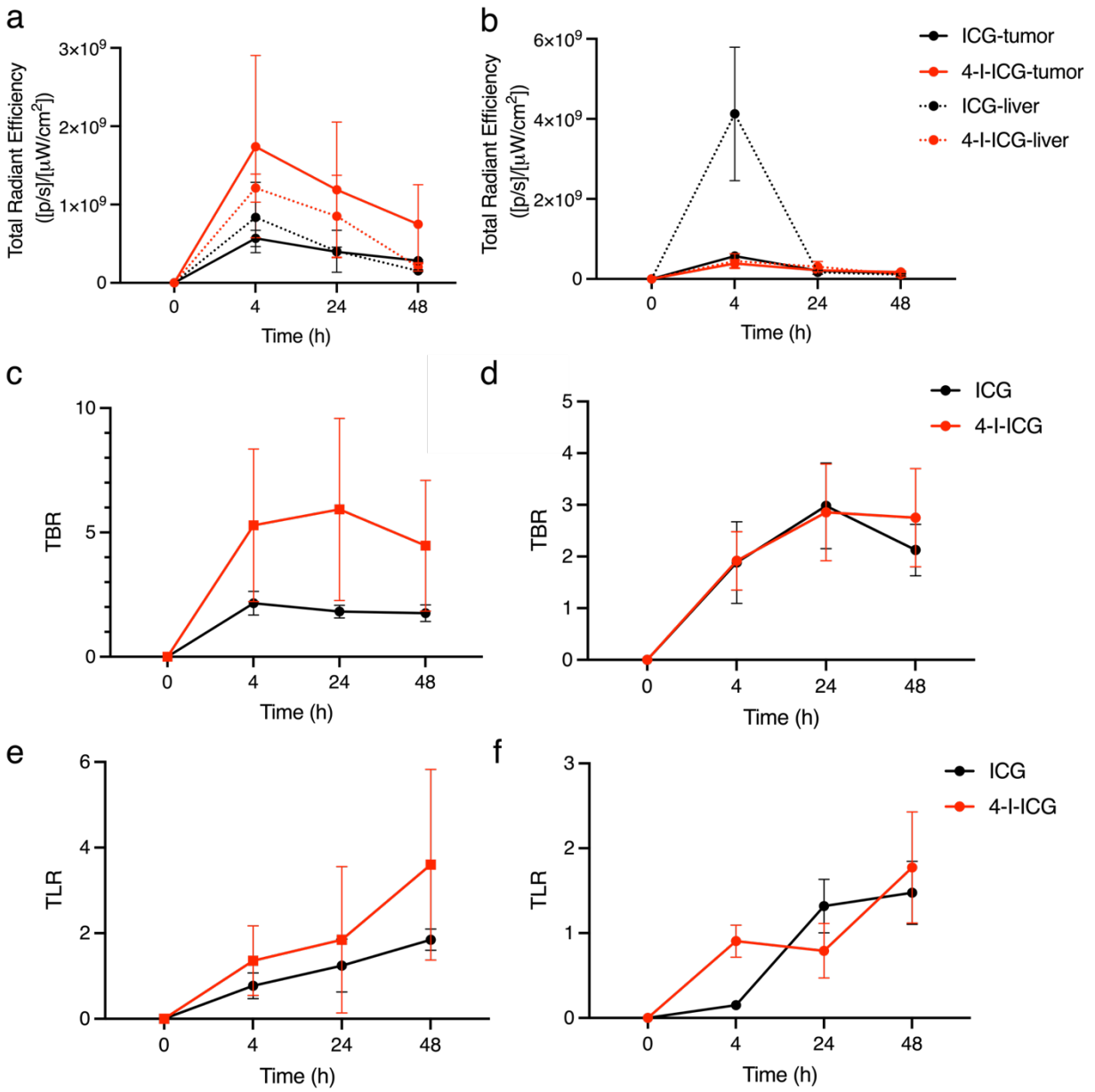

Figure S23. Total radiant efficiency of the tumors (solid lines) or livers (dashed lines) of **a.** Hep3B or **b.** Huh-7-tumor bearing athymic nude mice treated with ICG (2 mg/kg, black lines) or 4-I-ICG (2 mg/kg, red lines) over 48 h post-injection. Tumor-to-background ratios (TBRs) of **c.** Hep3B or **d.** Huh-7-tumor bearing athymic nude mice treated with ICG (2 mg/kg, black lines) or 4-I-ICG (2 mg/kg, red lines) over 48 h post-injection. Tumor-to-liver ratios (TLRs) of **e.** Hep3B or **f.** Huh-7-tumor bearing athymic nude mice treated with ICG (2 mg/kg, black lines) or 4-I-ICG (2 mg/kg, red lines) over 48 h post-injection.

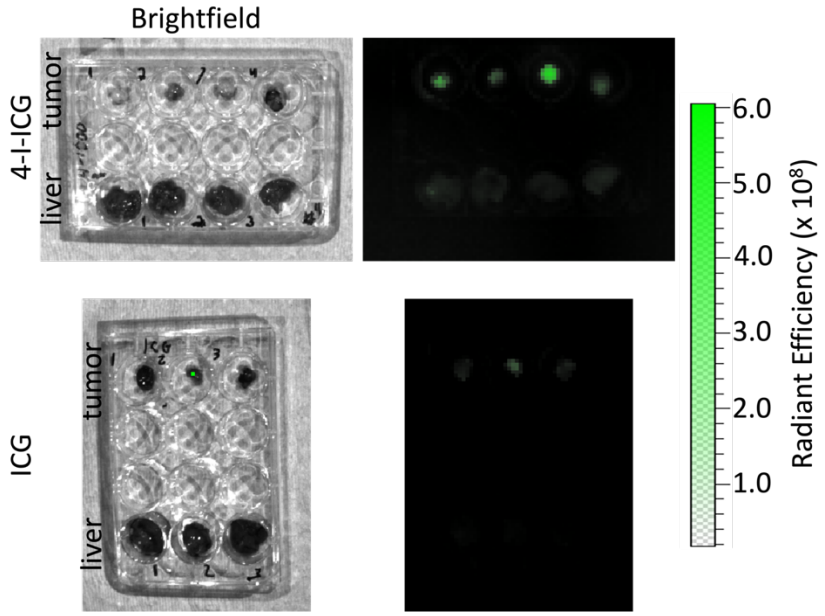

Figure S24. *Ex vivo* fluorescence images of Hep3B tumor-bearing mice intravenously injected with **4-I-ICG** (2 mg/kg) and **ICG** (2 mg/kg) after 48 h.

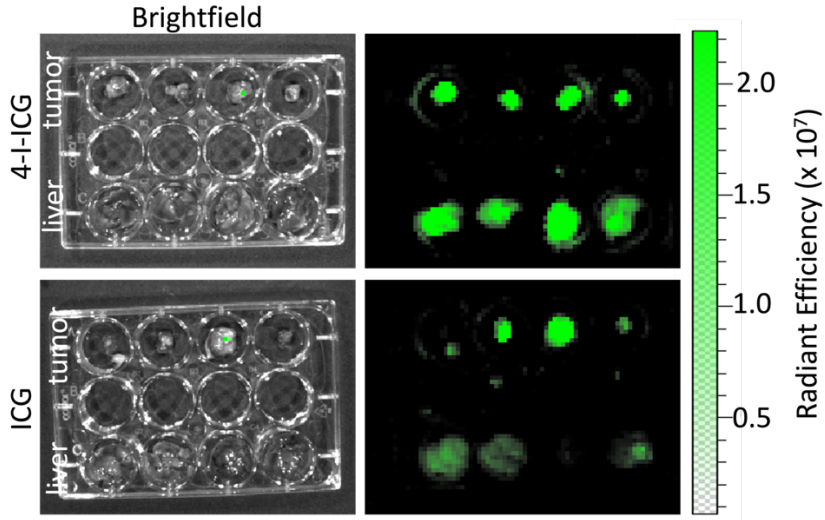

Figure S25. *Ex vivo* fluorescence images of Huh-7 tumor-bearing mice intravenously injected with **4-I-ICG** (2 mg/kg) and **ICG** (2 mg/kg) after 48 h.

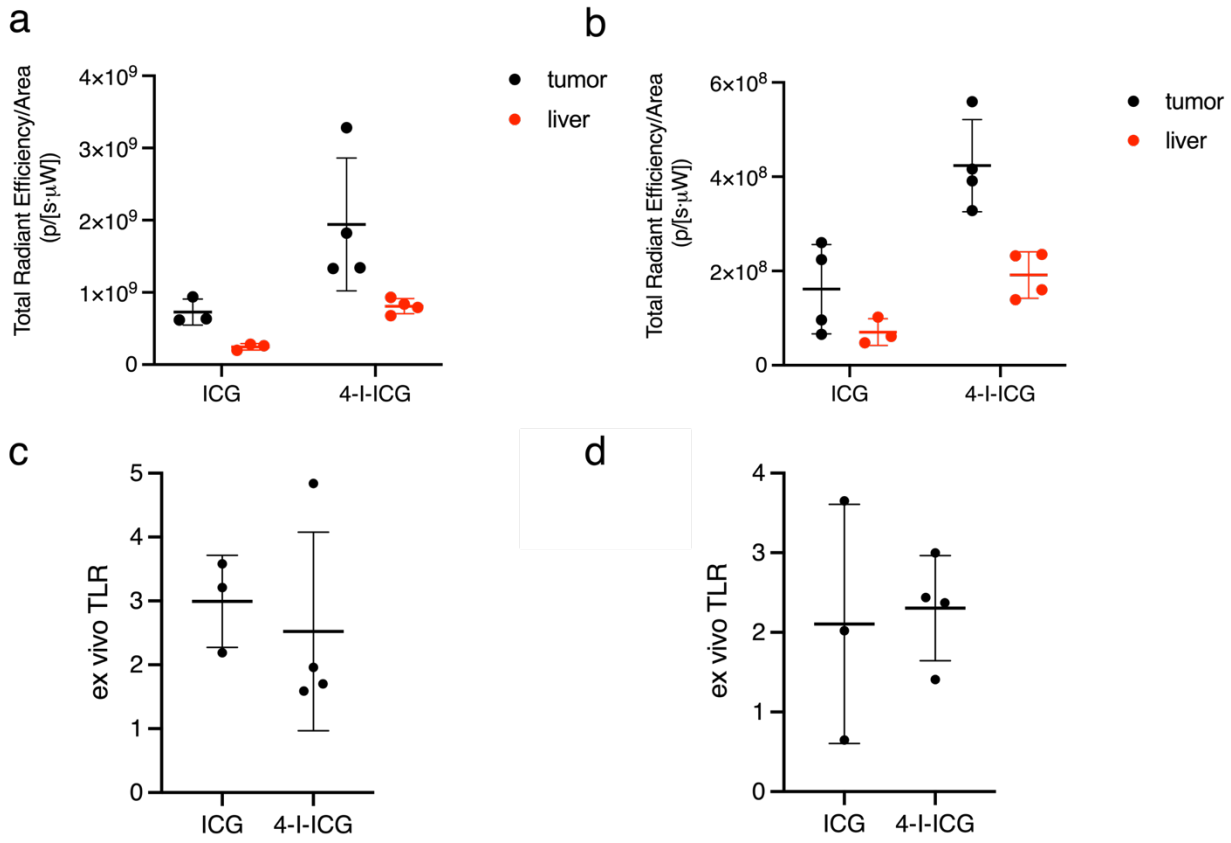

Figure S26. *Ex vivo* analysis of tumors (black dots) or livers (red dots) of **a.** Hep3B or **b.** Huh-7-tumor bearing athymic nude mice treated with ICG (2 mg/kg) or 4-I-ICG (2 mg/kg) at 48 h post-injection. *Ex vivo* TLRs of **c.** Hep3B or **d.** Huh-7-tumor bearing athymic nude mice treated with ICG (2 mg/kg) or 4-I-ICG (2 mg/kg) at 48 h post-injection.

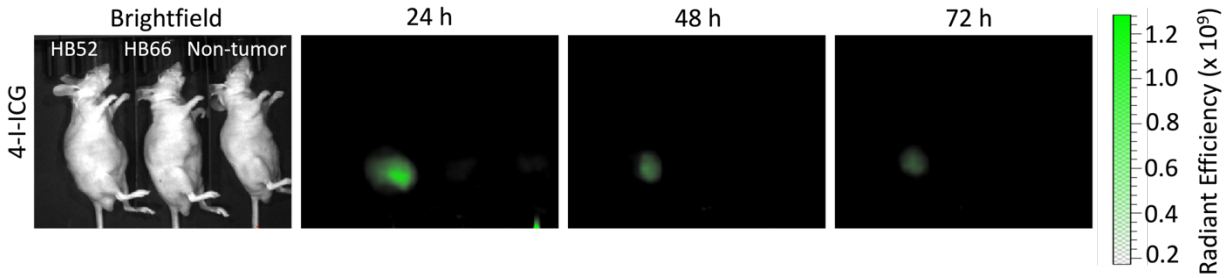

Figure S27. Side view of orthotopic PDX HB52, HB66, and non-tumor bearing (control) mice treated with **4-I-ICG** (10 mg/kg).

Compound 4-mono-I-ICG.

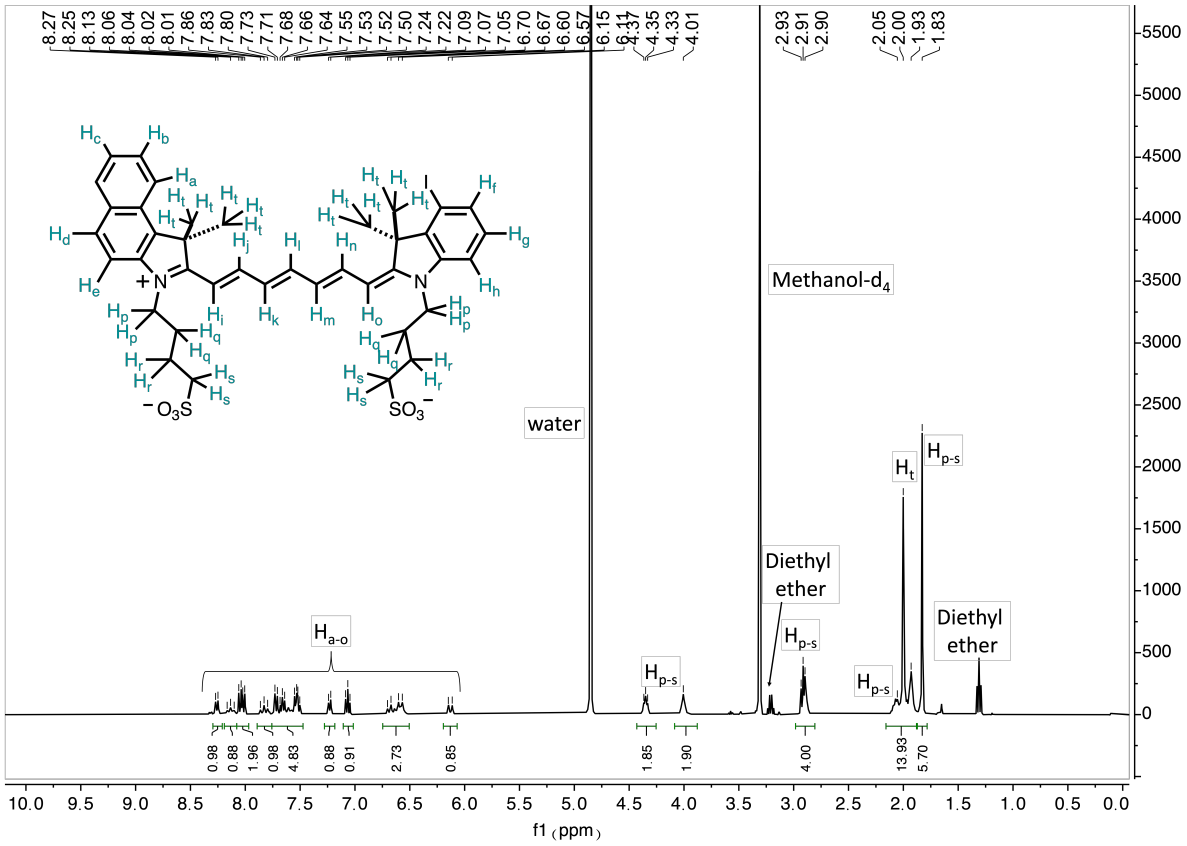

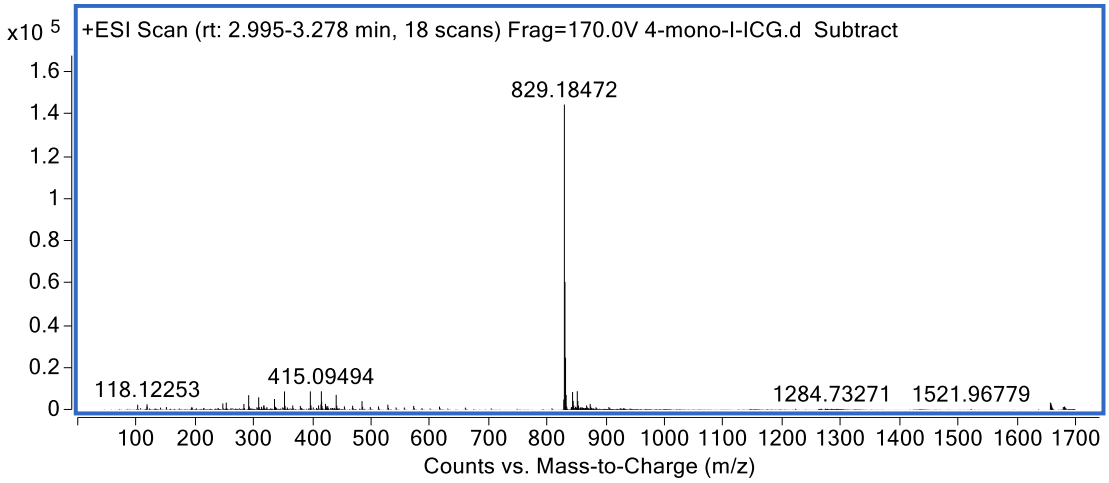

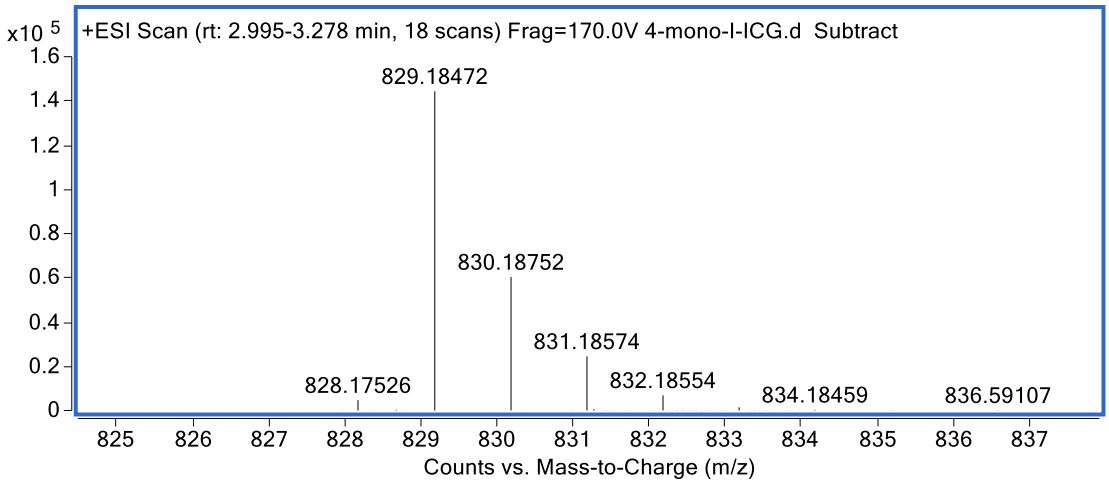
x10 5
+ESI Scan (rt: 2.995-3.278 min, 18 scans) Frag=170.0V 4-mono-I-ICG.d Subtract
1.6
1.4
1.2
1
0.8
0.6
0.4
0.2
0
829.18472
830.18752
831.18574
828.17526
832.18554
834.18459
836.59107
825
826
827
828
829
830
831
832
833
834
835
836
837
Counts vs. Mass-to-Charge (m/z)

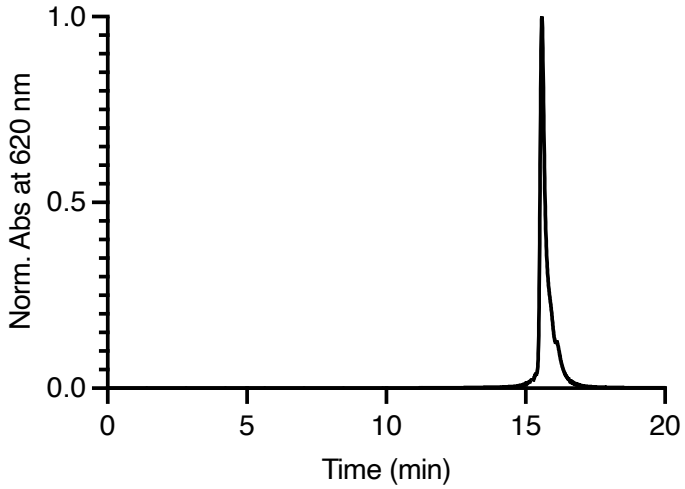
1.0
0.5
0.0
Norm. Abs at 620 nm
0
5
10
15
20
Time (min)

Compound 4-I-ICG.

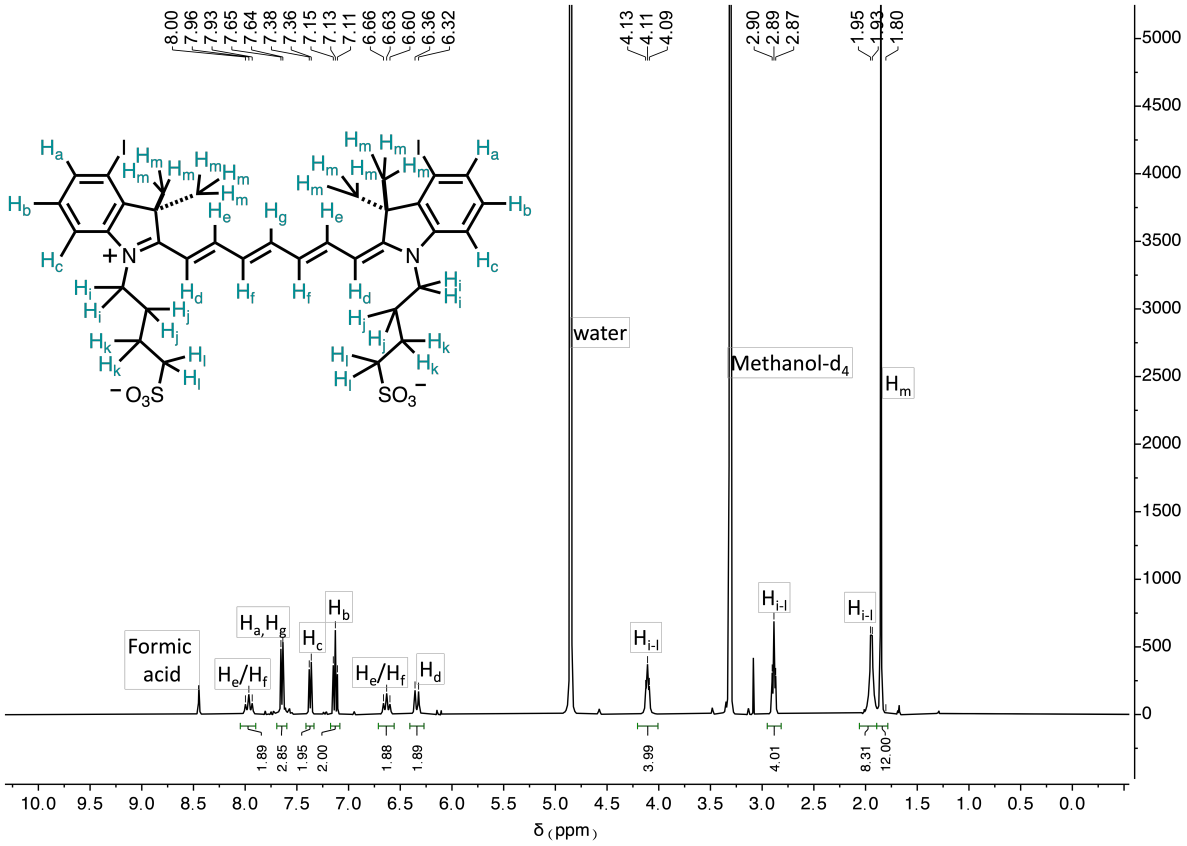

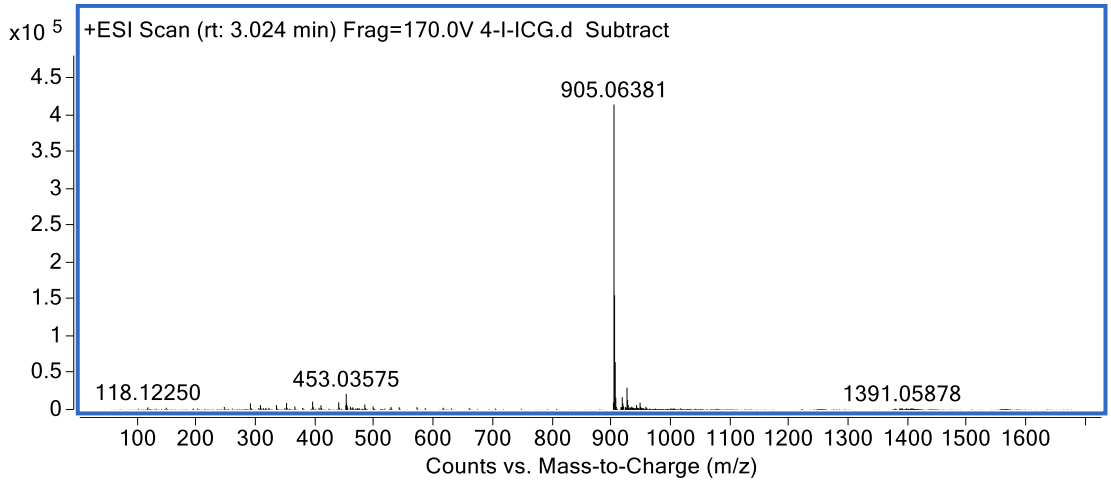

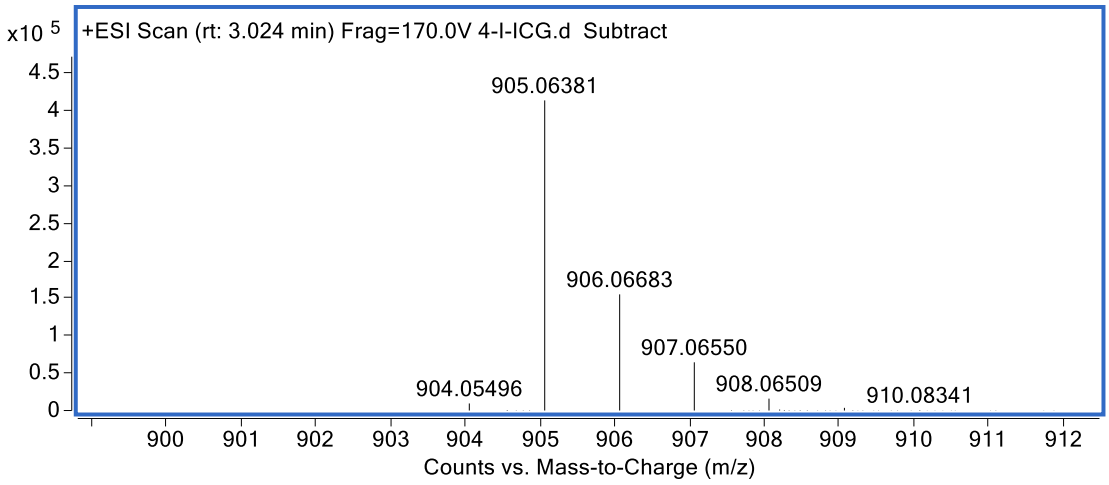
x10 5
+ESI Scan (rt: 3.024 min) Frag=170.0V 4-I-ICG.d Subtract
905.06381
906.06683
907.06550
908.06509
904.05496
910.08341
Counts vs. Mass-to-Charge (m/z)

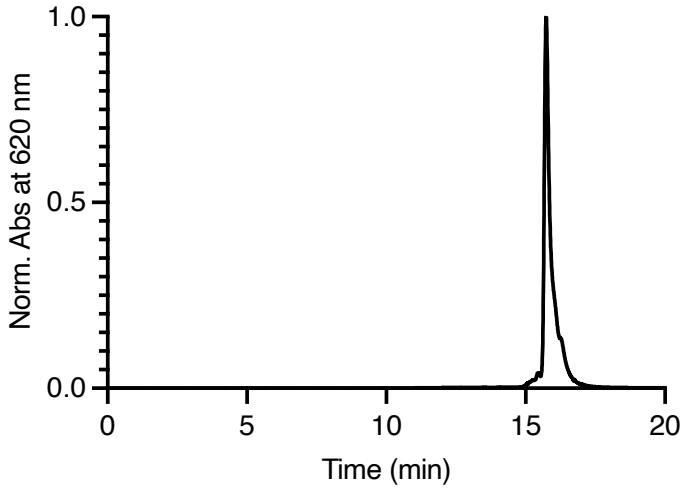
Norm. Abs at 620 nm
Time (min)

Compound 5-I-ICG.

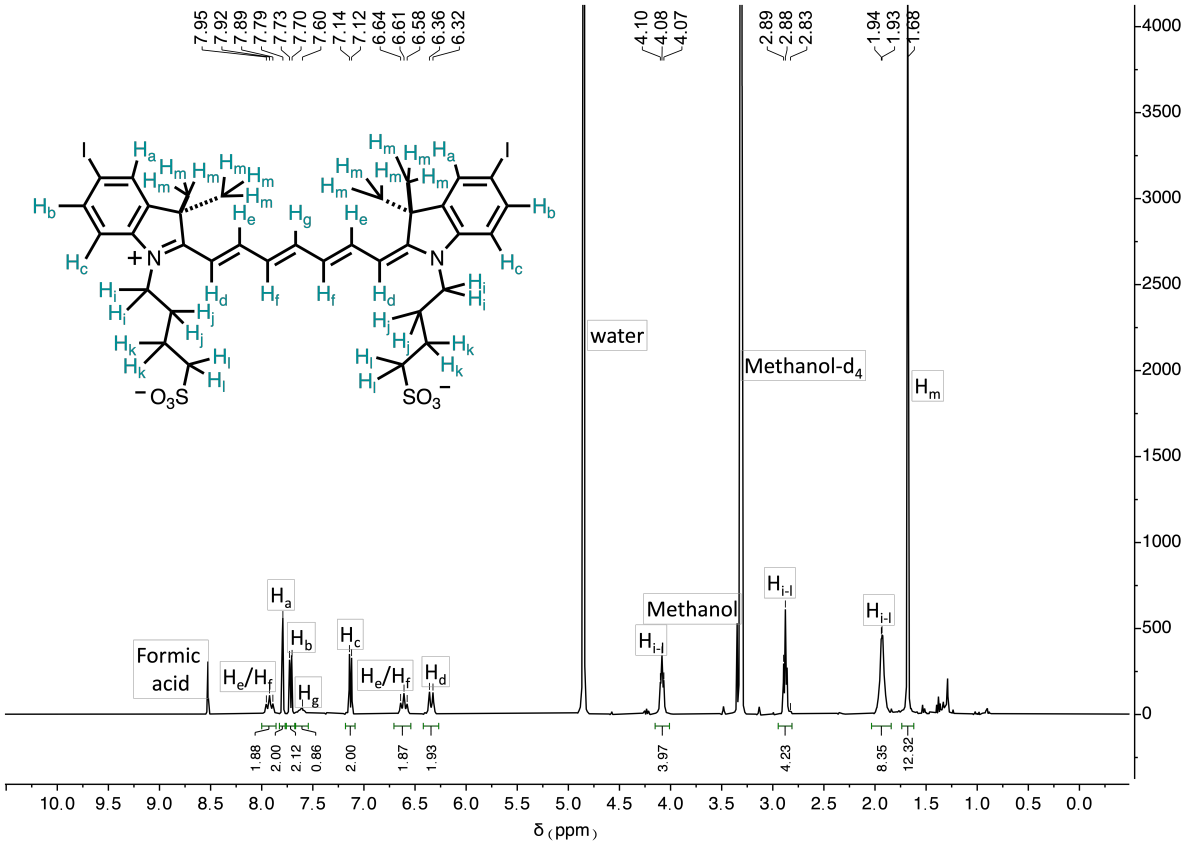

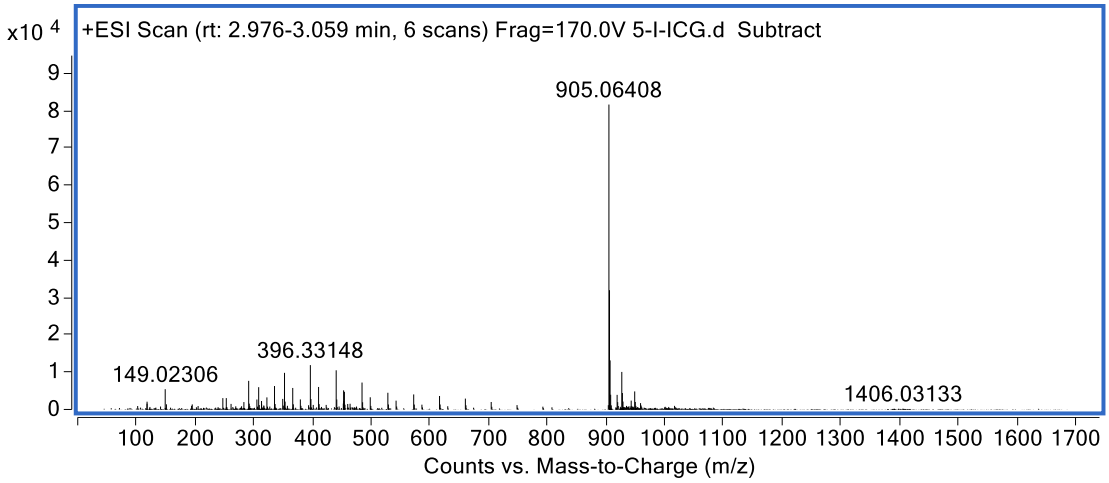

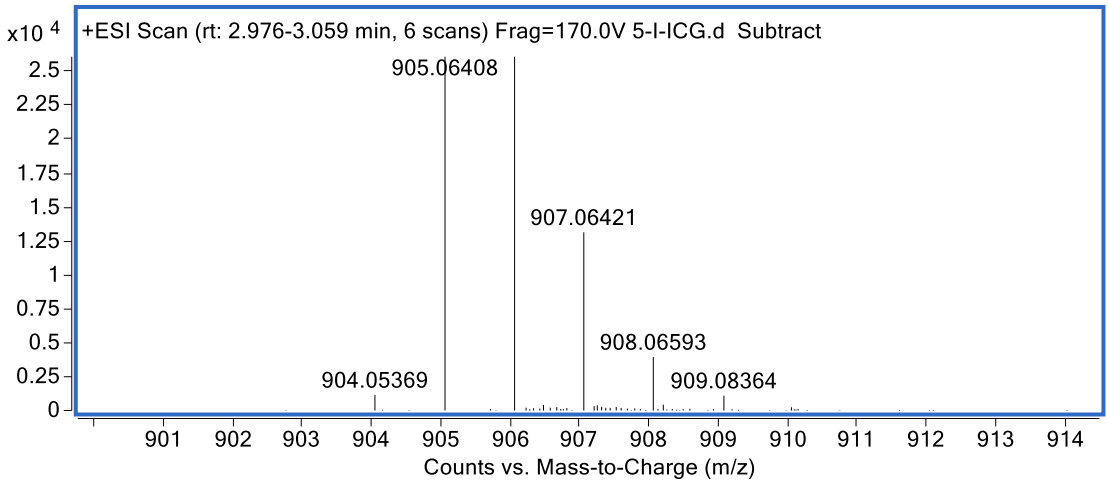
x10 4
+ESI Scan (rt: 2.976-3.059 min, 6 scans) Frag=170.0V 5-I-ICG.d Subtract
905.06408
907.06421
908.06593
904.05369
909.08364
Counts vs. Mass-to-Charge (m/z)

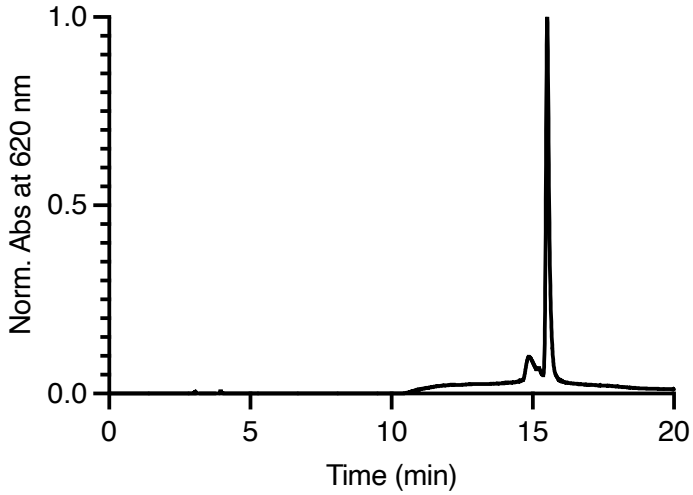
Norm. Abs at 620 nm
Time (min)

Compound 6-I-ICG.

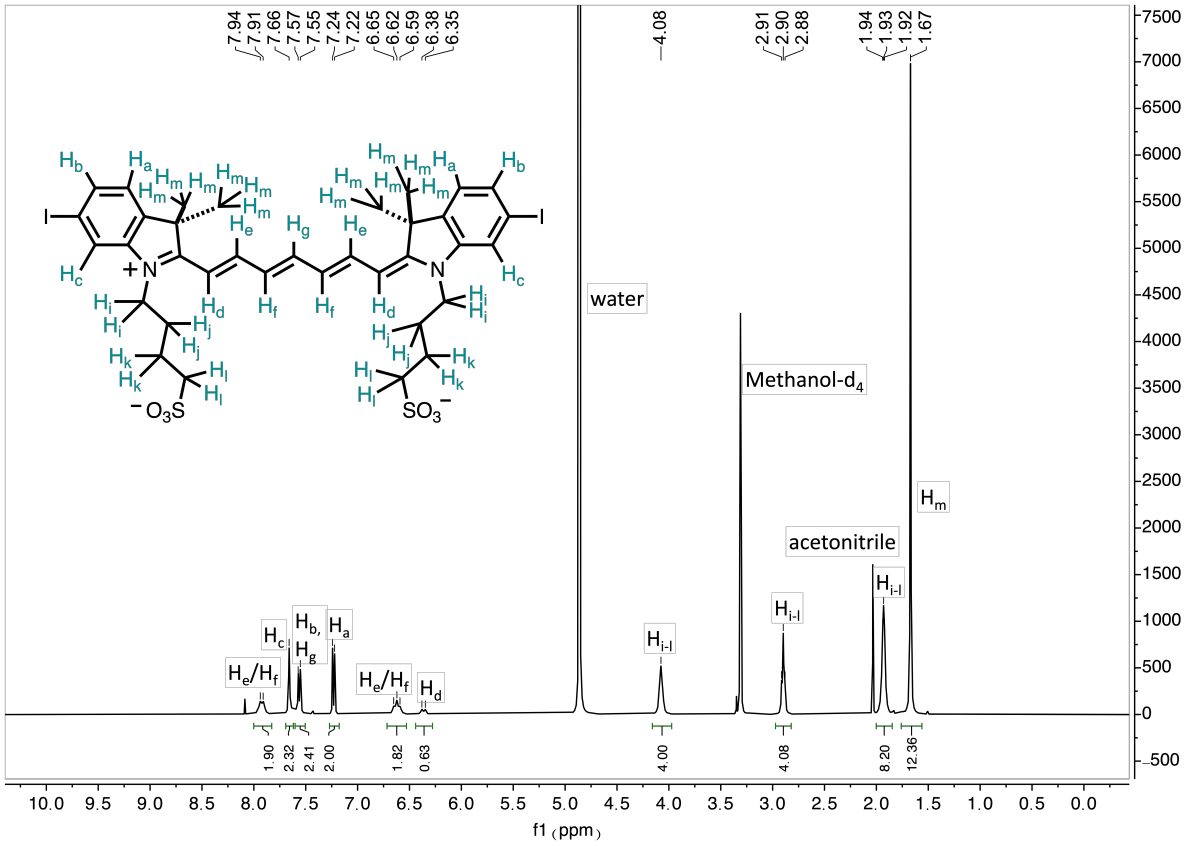

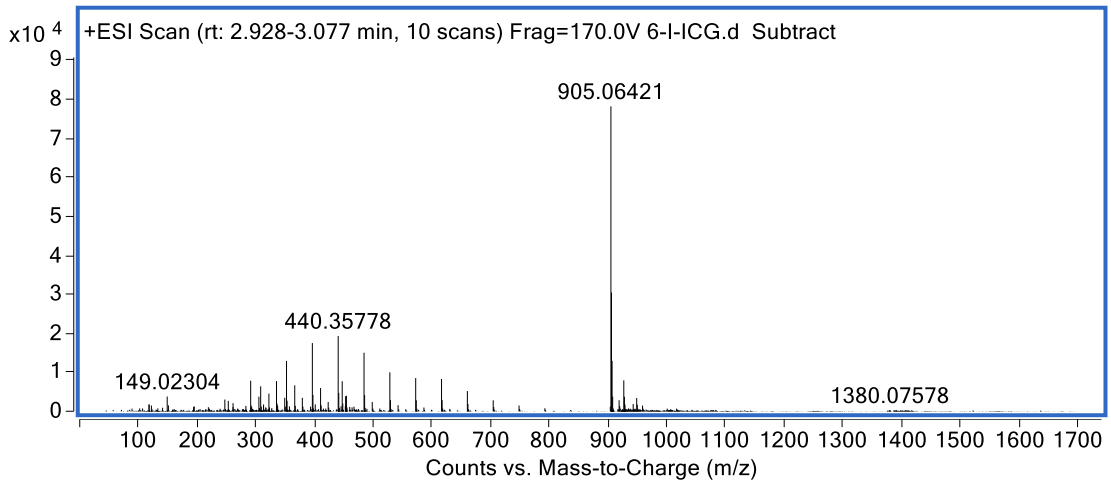

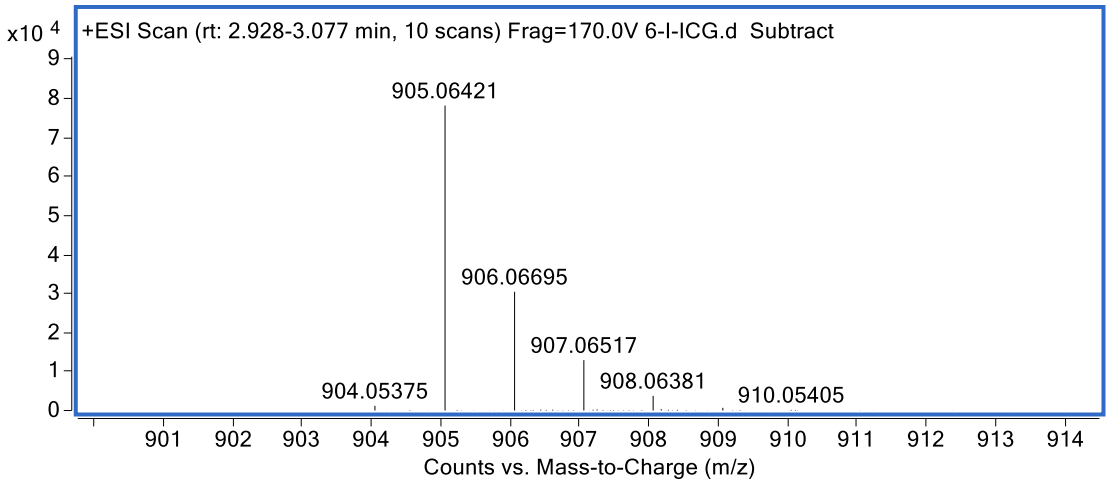

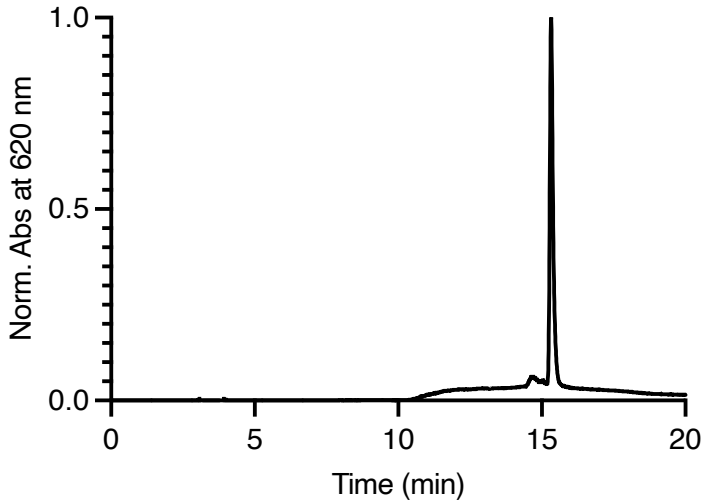

References.

(1) Wu, L.; Dai, Y.; Jiang, X.; Petchprayoon, C.; Lee, J. E.; Jiang, T.; Yan, Y.; Marriott, G. High-contrast fluorescence imaging in fixed and living cells using optimized optical switches. *PLoS One* **2013**, *8* (6), e64738. DOI: 10.1371/journal.pone.0064738

(2) Usama, S. M.; Marker, S. C.; Li, D. H.; Caldwell, D. R.; Stroet, M.; Patel, N. L.; Tebo, A. G.; Hernot, S.; Kalen, J. D.; Schnermann, M. Method To Diversify Cyanine Chromophore Functionality Enables Improved Biomolecule Tracking and Intracellular Imaging. *J Am Chem Soc* **2023**, *145* (27), 14647-14659. DOI: 10.1021/jacs.3c01765

(3) Park, S. J.; Kim, B.; Choi, S.; Balasubramaniam, S.; Lee, S. C.; Lee, J. Y.; Kim, H. S.; Kim, J. Y.; Kim, J. J.; Lee, Y. A.; et al. Imaging inflammation using an activated macrophage probe with Slc18b1 as the activation-selective gating target. *Nat Commun* **2019**, *10* (1), 1111. DOI: 10.1038/s41467-019-08990-9